Solar and wind assisted biohydrogen production from integrated anaerobic digestion and microbial electrolysis cell coupled with catalytic reforming.

Linus Onwuemezie, Hamidreza Gohari Darabkhani* h.g.darabkhani@staffs.ac.uk

Department of Engineering, School of Digital, Technologies and Arts (DTA), Staffordshire University, Stoke-on-Trent, ST4 2DE, UK

HIGHLIGHTS

- Dual-stage anaerobic digestion and microbial electrolysis are presented.
- Catalytic biogas reforming with CO_2 capture are modelled.
- Produced H_2 sales price is between \$2/kg and \$6/kg and the efficiency is ≥64%.
- For the proposed work, 1kg of produced H_2 can remove 10.92kg of atmosphere CO_2.
- Solar thermal and power and wind turbine systems replaced fossil fuels' combustion.

GRAPHICAL ABSTRACT

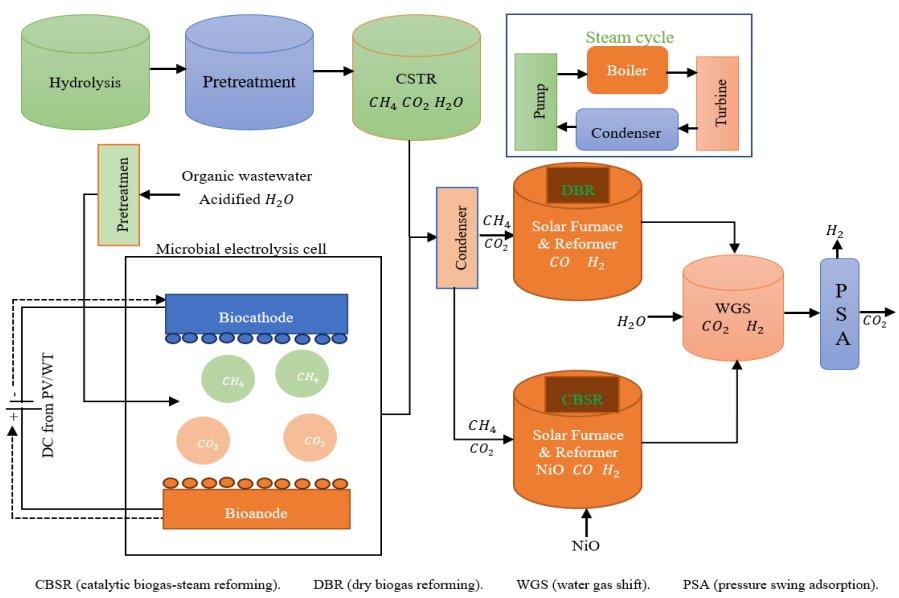

Abstract

To promote and improve the efficiency of biohydrogen production systems, an integrated AD and MEC (anaerobic digestion and microbial electrolysis cell) with catalytic syngas steam reforming (CSSR) was developed and simulated. This innovative integrated model predicts syngas formation from AD and MEC units, uses recovered heat for substrates pretreatment and solar parabolic dish (SPD) for heat source to decompose reformers' feeds. A combined 46 degradation reactions were used for acidogenesis, acetogenesis, and methanogenesis decomposition to predict syngas formation at different hydraulic retention time (HRT) and organic-loading rate (OLR). Biogas consisted of CH_4 and CO_2 from both AD and MEC were the CSSR feeds. The electric units of the hybrid system were powered by solar cells and wind turbine systems. The by-product CO_2 was captured and collected for underground storage. Controlled pH value, thermal pretreatment of AD and MEC digestates, and equilibrium feed rate improve overall efficiency by >5% with minimal volatile fatty acids (VFAs) and H_2S production. The results show that the developed system can accommodate both waste and biomass feeds with 64% system efficiency. The stated efficiency excluded power generation units (solar and wind). The H_2 sales price of this developed system is between \$2/kg and \$6/kg. However, by installing this proposed system in areas with more sunlight during the day, a further reduction in H_2 price is possible. Adopting this new proposed technology means that for every 1kg of produced H_2 using biomass plants as feedstock and replanting used feedstocks, 10.92kg of CO_2 can be removed from the atmosphere because plants fix and store CO_2 in their roots. Meanwhile, the proposed work encouraged the use of organic waste feedstock instead of agricultural products without replanting.

Keywords:

Solar parabolic dish (SPD); Solar cells and wind turbine systems; Anaerobic digestion (AD); Microbial electrolysis cell (MEC); Biomethane and biohydrogen production; Carbon neutrality.

Nomenclature

Abbreviations and Symbols

pH	Power of hydrogen
AD	Anaerobic digestion
CBSR	Catalytic biogas-steam reforming
CCS	Carbon capture and storage
CI	Conventional inert
CSP	Concentrating solar power
CSSR	Catalytic syngas steam reforming
CSTR	Control stirred tank reactor
DC	Direct current
DNI	Direct normal irradiance
DR	Dry reforming
DBR	Dry biogas reforming
Eq/Eqs	Equation/Equations
HX	Heat exchangers
HRT	Hydraulic retention time
HTF	Heat transfer fluid
$kg/month$	Kilo gram per month
$kmol/month$	Kilo mole per month
MEC	Microbial electrolysis cell
MENA	Middle East and North Africa
MW	Megawatt
NRTL	Non-random two-liquid
OLR	Organic loading rate
PDCs	Parabolic dish concentrators
PSA	Pressure swing adsorption
PSD	Particle size distribution
PV	Photovoltaic
SMR	Steam methane reforming
SPD	Solar parabolic dish
TS	Total solid
VFAs	Volatile fatty acids
VS	Volatile solid
WGS	Water gas shift
WT	Wind turbine
W/m^2	Watt per square metre

1. Introduction

Given that a significant amount of hydrogen (H_2) is produced from fossil fuel methods, H_2 production accounts for more than 2% of all global greenhouse gas (GHG) emissions. Thus, the production of hydrogen (H_2) from organic waste remains an effective way to reduce a carbon dioxide (CO_2) emission. The production of biohydrogen through biological methods such as indirect photosynthesis, anaerobic fermentation (AF), photo and dark and fermentation requires the involvement of hydrogenase enzymes found in microorganisms. NiFe hydrogenases are characterised by Fe and Ni ion based on their active site. Direct and indirect biophotolysis of H_2 production was considered the best alternative route for biohydrogen production due to the low volume of waste by-products [1]. On the contrary, an O_2 sensitivity of hydrogenases resulting in the poising of the active site and low efficiency of biophotolysis make anaerobic digestion (AD) and wastewater electrolysis the most promising routes for biohydrogen production. Solar and wind assisted AD and MEC (microbial electrolysis cell) coupled with catalytic syngas steam reforming (CSSR) can increase biogas production rate from organic waste and wastewater without a net increase in atmospheric CO_2.

In the AD pathway of syngas production, a group of bacteria work together to convert organic wastes into syngas mainly of methane (CH_4) and CO_2, and volatile fatty acid (VFA) [2]. Biochemical reactions of AD to produce biogas and VFA include hydrolysis, acidogenesis, acetogenesis and methanogenesis. Hydrolysis is the rate-limiting step as represented in Eq 1, while the acidogenesis step with chemical reactions written in Eq 2 employs acidogenic bacteria to degrade hydrolysis by-products including amino acids. As shown in Eq 3, acetogenesis uses acetic acid bacteria to produce acetate from organic acid, CO_2 and H_2. Anaerobic degradation of acetate from the methyl group and some of the VFA into CH_4, water (H_2O) and CO_2 is the final and methanogenesis step of the AD method [3]. Eqs 4 represents the chemical reactions of the methanogenesis pathway. AD method of biogas production is more energy efficient and has been considered a promising way to recover energy from organic waste. On the contrary, the main disadvantages of both AD and MEC are high VFA production, long start-up time, changes in operating conditions and impurities [4]. The nature of digestates, amount of total solid (TS) and volatile solid (VS), hydraulic retention time (HRT), organic-loading rate (OLR) and temperature are factors that influence the biogas conversion rate in the AD method. For instance, *Kondusamy & Kalamdhad.* [5] revealed that the use of young vegetative plants and small-size animal soil residues as feedstocks in an AD digester can reduce the amount of VFA by-products. Although, *Zhang, et al*. [6] reported a decrease in VFA amount and pH value during thermophilic pretreatment of AD feedstocks. Furthermore, *Hajizadeh et al.* [7] sensitivity analysis study of OLR and HRT shows that increasing the feeding rate above $1 l/kg$ reduces CH_4 formation. Nevertheless, a one-week incubation period for AD fermenters capable of producing 87% of CH_4 is acceptable for industries. However, *Aramrueang et al.* [8] mentioned that 30 days of incubation are required to reach 90% of CH_4 conversion efficiency which is not economically viable. Other factors that affect syngas production in the AD method are toxicity and power of

hydrogen (pH) value. For example, a pH value from 6.5 - 7.5 increases the production of biogas due to the activities of microorganisms in the digester [9].

$$\text{Hydrolysis} + H_2O \rightarrow C_2H_4O_2 + C_2H_5NO_2 + C_2H_6O + C_3H_6NO_2S + C_3H_7NO_2 + C_3H_7NO_3 + C_3H_8O_3 + C_4H_7NO_4 + C_4H_9NO_3 + C_5H_4O_2 + C_5H_9NO_2 + C_5H_9NO_4 + C_5H_{10}O_5 + C_5H_{11}NO_2 + C_6H_{13}NO_2 + C_6H_{14}N_4O_2 + C_9H_{11}NO_2 + C_{16}H_{34}O + C_{18}H_{34}O_2 + CO_2 + CH_4 + H_3N + H_2S + H_2O \quad (1)$$

$$\text{Acidogenic bacteria consume amino acid and hydrolysis by} - \text{products} \rightarrow C_2H_4O + C_2H_4O_2 + CH_3NO + C_3H_6O_2 + CH_4S + C_4H_8O_2 + C_5H_7NO_2 + C_5H_{10}O_2 + C_6H_6 + C_6H_6O + C_8H_7N + H_3N + CO_2 + H_2 + H_2S + H_2O \quad (2)$$

$$\text{Acetogenic bacteria consume acidogenic by} - \text{products} \rightarrow C_2H_4O_2 + C_3H_6O_2 + C_5H_7NO_2 + CO_2 + CH_4 + H_2 + H_3N \quad (3)$$

$$\text{Methanogenic bacteria consume acetogenic by} - \text{products} \rightarrow CH_4 + CO_2 + H_2O + VFA \quad (4)$$

The microbial electrolysis cell (MEC) can achieve a syngas (H_2, CH_4 and CO_2) production efficiency between 0.72 and 0.91 and use low external electricity and electrogenic microorganisms in bioelectrochemical reactions [10]. On the contrary, the presence of a membrane separator to separate H_2 from other by-products in dual-chamber MEC increases internal resistance, cost and membrane degradation [11]. Thus, mixed-culture MEC of methanogenic pathways has been considered as a possible solution to mitigate the drawbacks of dual-compartment MEC [12]. Another way to increase AD biogas production is the combination of both MEC and AD in a single unit. This approach can enhance syngas production with an applied voltage between 0.2 and 0.8 V. For example, *Anukam et al.* [13] mentioned that an integrated MEC and AD unit allows the transfer of exoelectrogens to the AD fermenter, resulting in higher CH_4 formation and lower VFA by-product. However, *Lee et al.* [14] argued that the approach of combining AD and MEC methods to boost biogas production requires further research as a decrease in biogas formation was seen after the third cycle. Furthermore, chemical, thermal, biological, and other pretreatment processes of AD and MEC digestates can increase syngas production [15]. For example, using thermal hydrolysis pretreatment of AD feedstocks, an increase in biogas formation was observed because of improved degradation kinetic, digestate solubilisation and access to more feed rate [16]. However, *Climent et al.* reported that high-temperature pretreatment of AD feedstock does not influence syngas production, while the findings of *Carrère et al* show that up to 150% increase in biogas production can be achieved using high-temperature pretreatment [17] [18]. Furthermore, *Wang & Lee*. [19] investigated work showed improved syngas production of AD and MEC methods by using renewable energy sources, dual anaerobic digesters, co-digestion and optimisation of the operating parameters. Nonetheless, higher electricity usage by AD and MEC digesters and the increase in biogas purification costs are disadvantages of such improvement methods [4]. Thus, *Hajizadeh et al* proposed a combined dry reforming (DR) and AD methods to enhance syngas production and separate H_2 from other by-products [7]. The efficiency of the investigated work was 0.73 at a H_2 selling price of $1.39/kg. Eqs 5 – 7 represent the electrochemical reaction pathways of MEC in syngas production.

$$CH_3COOH/C_2H_4O_2 + 2H_2O \rightarrow 2CO_2^- + 8H^+ + 8e^- \ (Anode) \quad E^0 = -0.28V \ vs \ SHE \ \text{(standard hydrogen electrode)} \quad (5)$$

$$2CO_2^- + 8H^+ + 8e^- \rightarrow 4H_2 \ (Cathode) \quad E^0 = -0.24V \ vs \ SHE \quad (6)$$

$$CH_3COOH/C_2H_4O_2 + 2H_2O \rightarrow 2CO_2 + 4H_2 \quad E^0 = -0.52V \ (Overal) \quad (7)$$

Dry reforming (DR) uses light hydrocarbon or biogas of AD as reformer feedstock and steam addition in water gas shift (WGS) units to produce H_2 and CO_2 by-products. This process requires the use of precious metal catalysts or bimetallic Ni-Co catalysts in the reformer to prevent catalyst deactivation because of carbon deposition on the active site [20]. Unlike the DR process of H_2 production, catalytic biogas-steam reforming (CBSR) with NiO catalyst involves the reaction of light hydrocarbon to produce synthetic gas and regeneration of NiO catalyst before by-product CO_2 capture [21]. Our previous work investigated hydrocarbon reforming with NiO as a reforming catalyst in process simulation, with findings showing higher syngas production at lower operating temperature compared to SMR (steam methane reforming) [22]. Furthermore, an integrated SMR and DR to reconvert by-product CO_2 to CO has been studied with findings showing higher exergy loss in the reformer. The exergy destruction in both SMR and DR methods was 80.06% and 70.49%. However, exergy loss in the combustion process for DR was higher due to the endothermic nature of the process [23]. Since the combustion of fossil fuels in the reformer furnace promotes greater exergy destruction and carbon emissions, the use of renewable thermal energy sources for feedstock decomposition can reduce such losses and improve the overall efficiency of both reforming processes. For

instance, earlier studies show that thermal energy from a CSP plant can replace fossil fuels' combustion in a decomposer furnace with oxy-hydrogen combustion to compensate for losses [24]. In addition, between 20 and 91kg/d of H_2 can be produced by electrolysis of H_2O using a single Gamesa G47 turbine and Photovoltaic (PV) systems in Zahedan Iran [25]. Electricity produced from a wind turbine system can also be used for H_2O and wastewater electrolysis. Nonetheless, the electrochemical splitting of H_2O and wastewater molecule into H_2, O_2 and other by-products with the usage of photon energy is considered more efficient than wind energy [26]. CBSR chemical reactions for H_2 production, WGS and CO_2 capture are represented in Eqs 8 – 11.

$$CH_4 + CO_2 \rightarrow 2CO + 2H_2 \quad (8)$$

$$CH_4 + CO_2 + NiO \rightarrow 2CO + 2H_2 + NiO \quad (9)$$

$$CO + H_2O \rightarrow CO_2 + H_2 \quad (10)$$

$$CaO + CO_2 \rightarrow CaCO_3 \quad (11)$$

Concentrating solar power (CSP) converts photon energy into thermal energy by collecting and reflecting the irradiance of the sun at the focal point. CSP operating with a Ranking cycle and thermal energy storage (TES) can generate electrical energy when the sun is unavailable. Parabolic dish concentrators (PDC), solar energy tower (SET), parabolic trough collectors (PTC) and linear Fresnel collectors (LFC) are the four main types of CSP technology. Among other CSP systems, *Karimi et al.* stated that PDC produces the most thermal energy and operates at higher efficiency compared to others [27]. Although the installation of CSP systems in MENA (Middle East and North Africa) regions has been suggested as another possible way of efficiency improvement as MENA countries experience more sunshine during the day [28].

Integrated solar dish and Stirling engine for sustainable and renewable electricity generation for rural electrification was studied by *Kalogirou.* [29] and reported an efficiency of 29%. *Sookramoon1 et al.* [30] also reported a lower efficiency (26.2%) of a combined solar dish and Stirling engine by concentrating the solar radiation from the dish to the receiver with a mounted Stirling engine. Solar parabolic dish (SPD) configured with polished stainless steel, anod aluminium and polymer film absorbing materials, and operating with air, H_2O and therminol VP-1 as the working fluids were investigated. The studied work reported an efficiency of 35% on SPD operating with H_2O as the working fluid. The recorded efficiency of SPD operating with H_2O as the working fluid was attributed to the good absorbing coefficient in the tube [31]. In addition, at a lower irradiance of $725\ W/m^2$ for the hybrid solar dish and Stirling engine, an overall system efficiency of 17.6% was reported [32]. To improve the efficiency of SPD, *Castellanos et al.* [33] developed a mathematical model with an integrated solar tracking system. The developed system with an exit working fluid temperature of 1322.85°C achieved an efficiency of 88% for the dish concentrator and 90% for the receiver. However, the maximum efficiency reported was 30%. In addition to the integrated solar dish and Stirling engine for electricity generation, a combined photoelectrochemical method of H_2 production was investigated with findings showing efficiency >20%. [34]. Despite the advantages of CSP systems, such as thermal energy storage and good operating performance, the photovoltaic (PV) system is considered more economically feasible [35]. On the contrary, limited hours of sunshine during the winter period make wind energy more attractive in Western nations. For example, *Laha & Chakraborty* [36] affirmed that offshore wind can reduce the carbon footprint without increasing upfront costs. Most Western countries like the United Kingdom (UK) rely on offshore and onshore wind energy systems to achieve net-zero carbon emissions by 2050 [37].

To promote sustainable and efficient biohydrogen production, this study proposed a renewable-powered hybrid AD and membraneless MEC system with thermally pretreated digestates for biogas production and DBR or CBSR for biohydrogen production. As low H_2 production is associated with anaerobic fermentation (AF) and recovery of H_2 from other by-products increases operating costs due to high membrane cost and internal resistance of gas cross-over, a methanogenic pathway of biogas (CH_4) production was considered. The introduction of MEC was another means of maximising CH_4 production rate which is one of the reformer feedstocks. Incorporating reforming methods with WGS units represents the best approach for reducing H_2 sales price and increasing H_2 yield. In addition, the proposed integrated systems utilised PDC for thermal decomposition of reformers' feeds, solar or wind to power the electrical units and recovered heat for hydrolysed substrate pretreatment. To improve the proposed system efficiency and remove carbon emissions from the process, oxy-hydrogen combustion in the reformer furnace to compensate for heat loss, CO_2 capture by absorption and the application of the steam cycle were covered. Fig. 1a displays a simplified diagram of the proposed hybrid system.

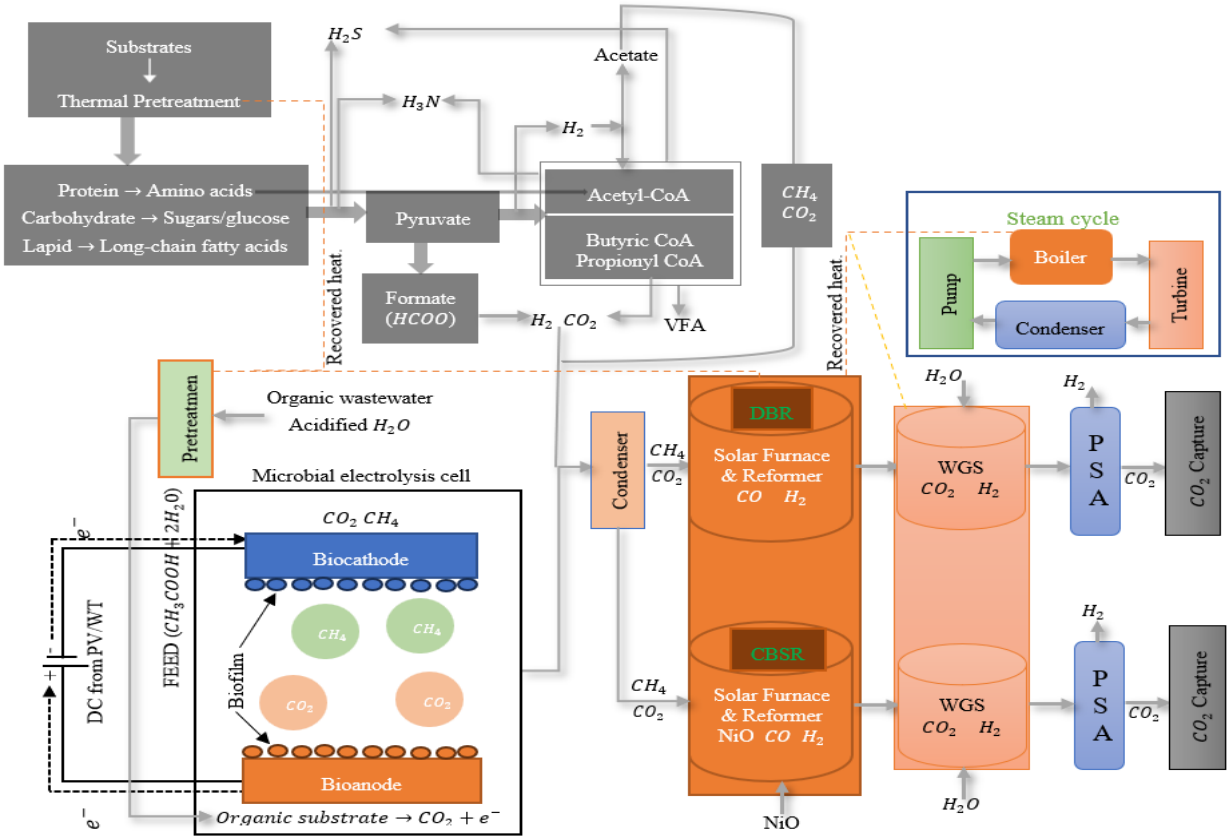

Fig 1a: Solar or wind powered integrated AD, MEC and DBR or CBSR systems, coupled with a steam cycle for H_2 production.

2. Material and simulation method

Organic wastes and wastewater were among the list of materials used for biogas production in both AD and MEC processes. Unlike other waste feedstocks with 10.86 – 25.95% total solid (TS) and 10.22 - 24.59% volatile solid (VS) [38], the AD unit of this study utilised ≤27% TS of the complex organic waste substrates. The stated TS value was considered to allow the flexibility and utilisation of this proposed system in waste and non-waste treatment plants since a higher TS value decreases the yield of biosynthetic gas. In solid-state AD plants, between 20% and 40% TS content is allowed. While a wet AD uses >15% TS to accommodate substrate flexibility and lower investment and operation costs [39]. A wet AD is utilised in this study because of the decreased TS value after particle size reduction and thermal pretreatment of the utilised substrates. The mixed substrate feed in this study contains protein, carbohydrate and lipid to produce amino acids, sugar/glucose and long-chain fatty acids in the hydrolysis stage. To model the hydrolysis stage in a process simulation such as Aspen Plus, new materials were added to the datasheet. Combined 46 chemical decomposition reactions for hydrolysis, acidogenesis, acetogenesis and methanogenesis were implemented to produce biogas feed for the reforming technologies. The separate extent of reaction of the rate-limiting step (hydrolysis) was set between 0.0001 and 1.0 to establish the effect of substrate pretreatment. Other types of components used during the property setup were solid and conventional. Mixed and conventional inert (CI) substreams and normal distribution function type of logarithmic mesh particle size distribution (PSD) were applied. A smaller substrate size was utilised, which is another form of feed pretreatment to reduce the TS value. Non-random two-liquid (NRTL) and Peng-Robinson equation of states were the property methods used because of the presence of charged species and the complexity of the model.

2.1 Overview of AD and MEC for biogas production.

AD hydrolysis was simulated using a separator and Gibbs reactor blocks to obtain the stoichiometric data for the first stage of the process. The extent of the hydrolysis reaction and by-products is illustrated in Table 1. The acidogenesis of AD which involves the degradation of simple sugar, amino and fatty acids was simulated using separation blocks, Gibbs reactor blocks and a control stirred tank reactor (CSTR). Using Gibbs reactors, the correct stoichiometric values were obtained for the reactants

and products for the CSTR decomposition reaction. AD acetogenesis converts acidogenesis by-products into acetic acid, H_2, and CO_2 in the same CSTR using acetogenesis bacteria. A second CSTR was used in the final stage of the AD process to maximise the biomethane production. Initially, the Gibbs reactor was used to elucidate the specific components of the reactions in the methanogenesis phase. Using the Gibbs reactor, the possible compositions of the product elements were investigated. A modified Fortran code of calculator blocks from *Haider & Smith*. [40] were implemented for pH inhabitation and temperature dependency under mesophile and thermophile conditions. The by-product of hydrolysis, acidogenesis, acetogenesis and methanogenesis of AD is shown in Fig. 1b. Unlike the AD process, the MEC used a Gibbs reactor with an electrolyte chemical ID defined in Eqs 5 – 7 to produce more biogas feed for reforming methods.

Table 1: AD hydrolysis reaction and products.

No:	Component ID	Type	Component Name	Alias
1.	Cellulose	Solid	Dextrose	$C_6H_{12}O_6$
$C_6H_{12}O_6 + H_2O \rightarrow 2C_2H_6O + 2CO_2$				
2.	Hemicellulose	Solid	Glutaric-Acid	$C_5H_8O_4$
$C_5H_8O_4 + H_2O \rightarrow 2.5C_2H_4O_2$ $C_5H_8O_4 + H_2O \rightarrow C_5H_{10}O_5$				
3.	Acetic-Acid	Conventional	Acetic-Acid	$C_2H_4O_2$
4.	Xylose	Conventional	Xylo-pyranose	$C_5H_{10}O_5$
$C_5H_{10}O_5 \rightarrow C_5H_4O_2 + 3H_2O$				
5.	Furfural	Conventional	Furfural	$C_5H_4O_2$
6.	Ethanol	Conventional	Ethanol	C_2H_6O
$2C_2H_6O + CO_2 \rightarrow 2C_2H_4O_2 + CH_4$				
7.	Protein/Soluble Protein	Pseudo Component	Protein	$C_{13}H_{25}O_7N_3S$
$C_{13}H_{25}O_7N_3S + 6H_2O \rightarrow 6.5CO_2 + 6.5CH_4 + 3H_3N + H_2S$				
8.	Insoluble protein	Pseudo Component	Insoluble Protein	$C_{13}H_{25}O_7N_3S$
$C_{13}H_{25}O_7N_3S + 0.3337H_2O \rightarrow 0.045C_6H_{14}N_4O_2 + 0.048C_4H_7NO_4 + 0.047C_4H_9NO_3 + 0.172C_3H_7NO_3 + 0.074$ $C_5H_9NO_4 + 0.111C_5H_9NO_2 + 0.25C_2H_5NO_2 + 0.047C_3H_7NO_2 + 0.067C_3H_6NO_2S + 0.074C_5H_{11}NO_2 + 0.07C_6H_{13}$ $NO_2 + 0.046C_6H_{13}NO_2 + 0.036C_9H_{11}NO_2$				
9.	Arginine	Conventional	Arginine	$C_6H_{14}N_4O_2$
10.	Aspartic-acid	Conventional	Aspartic-acid	$C_4H_7NO_4$
11.	Threonine	Conventional	Threonine	$C_4H_9NO_3$
12.	Serine	Conventional	Serine	$C_3H_7NO_3$
13.	Glutamic-Acid	Conventional	Glutamic-Acid	$C_5H_9NO_4$
14.	Formyl-morpholine	Conventional	Formyl-morpholine	$C_5H_9NO_2$
15.	Nitroethane	Conventional	Nitroethane	$C_2H_5NO_2$
16.	Alanine	Conventional	Alanine	$C_3H_7NO_2$
17.	Cysteine	Pseudo Component	Cysteine	$C_3H_6NO_2S$
18.	Valine	Conventional	Valine	$C_5H_{11}NO_2$
19.	Leucine	Conventional	Leucine	$C_6H_{13}NO_2$

20.	Phenylalanine	Conventional	Phenylalanine	$C_9H_{11}NO_2$
21.	Triolein	Conventional	Triolein	$C_{57}H_{104}O_6$
$C_{57}H_{104}O_6 + 3H_2O \rightarrow C_3H_8O_3 + C_{18}H_{34}O_2$				
22.	Glycerol	Conventional	Glycerol	$C_3H_8O_3$
23.	Oleic-Ac	Conventional	Oleic-Acid	$C_{18}H_{34}O_2$
24.	Tripalmitin	Conventional	Tripalmitin	$C_{51}H_{98}O_6$
$C_{51}H_{98}O_6 + 8.436H_2O \rightarrow 4C_3H_8O_3 + 2.43C_{16}H_{34}O$				
25.	Hexadecanol	Solid	Hexadecanol	$C_{16}H_{34}O$
26.	Palmito-Olein	Pseudo Component	Palmito-Olein	$C_{37}H_{70}O_5$
$C_{37}H_{70}O_5 + 4.1H_2O \rightarrow 2.1C_3H_8O_3 + 0.9C_{16}H_{34}O + 0.9C_{18}H_{34}O_2$				
27.	Palmito-Linolein	Pseudo Component	Palmito-Linolein	$C_{37}H_{68}O_5$
$C_{37}H_{68}O_5 + 4.3H_2O \rightarrow 2.2C_3H_8O_3 + 0.9C_{16}H_{34}O + 0.9C_{18}H_{32}O_2$				

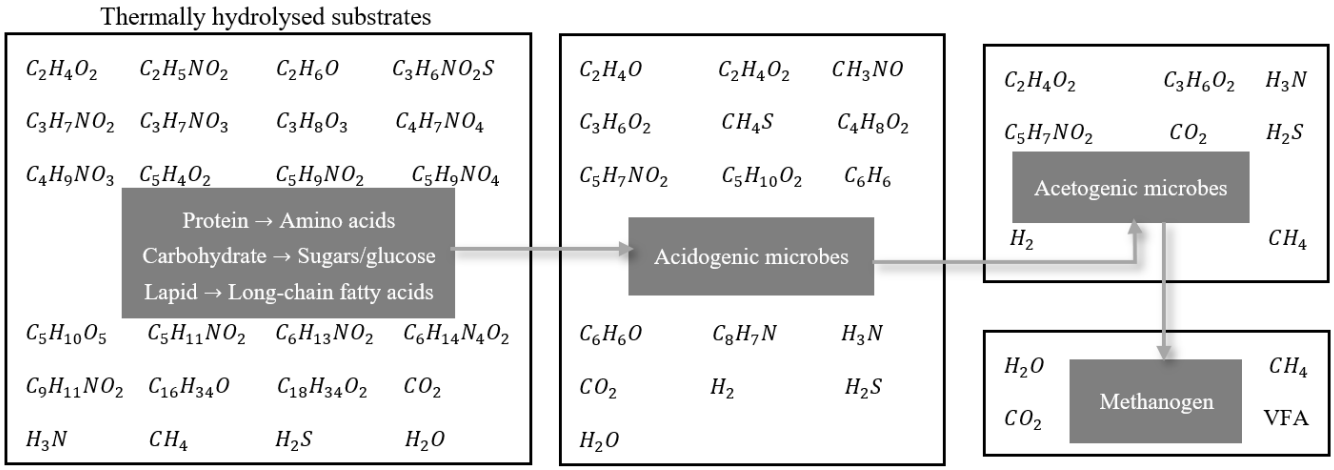

Fig 1b: Hydrolysis, acidogenesis, acetogenesis and methanogenesis by-products of AD in the digester.

2.2 Overview of DBR and CBSR for biohydrogen production, SPD, solar cells and wind turbine (WT) systems.

AD and MEC biogas (CO_2 and CH_4) are fed to both DBR and CBSR reformers to produce H_2 and convert CO_2 to carbon monoxide (CO). The introduction of WGS enabled the conversion of CO back to CO_2 and increased the H_2 production rate. Distinct from the sorption enhanced–chemical looping, which requires the use of 2 reformers to reduce NiO to Ni and regenerate NiO, this study enabled the reduction and regeneration of NiO catalyst in a single reformer. The downstream unit which is pressure swing adsorption (PSA) separates H_2 from CO_2 at a high purity.

The solar thermal system was modelled in CAD (computer-aided design) and simulated in Ansys fluent, whereas both solar cells and WT systems for electricity generation were developed in Simulink. In the Simulink environment, the final stage of connecting the Aspen Plus model (AD and MEC coupled with DBR or CBSR) to the renewable energy systems was completed as both software interfaces with one another. Table 2 lists the main input parameters of SPD, solar cells and WT systems.

Table 2: Design parameters for Solar parabolic dish (SPD), wind Turbine (WT) and solar cell (SC).

Solar parabolic dish (SPD)			
Parameters	Value	Parameters	Value
Dish and receiver design parameters		Working fluid properties	
Design point DNI	600 -1200 W/m^2	Working fluid	CH_4 & CO_2
Hot/loop exit HTF temperature	1000 - 1300°C	HTF density	2.637kg/m^3

Cold/loop intake HTF temperature	240 - 350°C	Flow rate of the working fluid	0.8kg/hr
Receiver thermal efficiency	0.86	Heat transfer properties	
Solar dish reflective area	159653.06 mm^2	Tube inner diameter	4.4mm
Solar dish reflective volume	1416940.85 mm^3	Tube thickness	1mm
Wind turbine parameters		Solar cell parameters	
Parameters	Value	Parameters	Value
Rated power	3000W	Rated power	3000W
Maximum cp	0.45	Array type	Roof mount
Cut-in wind speed	4m/s	Tilt	0°
Cut-off wind speed	25m/s	Azimuth	180°
Total system loss	18%	Total system loss	14%

2.3 Process simulation of integrated AD and MEC coupled with DBR and CBSR.

Aspen Plus process simulation software was used to develop and simulate a combined AD, MEC and DBR and an integrated AD, MEC and CBSR with a non-random two-liquid (NRTL) equation of states solver. Apart from the presence of charged species in AD and MEC, the NRTL equation of state allows the physical and chemical equilibrium of the model to be correctly predicted. Peng-Robinson is another equation of state solver used for DBR and CBSR simulation. The ideal gas property and steam-table free water methods were also used to adjust and accommodate pressure deviation. The assumptions considered in the process simulation for both integrated systems are listed below:

- Steady-state condition for entire the process.
- Heat and pressure losses are estimated.
- CSTR temperature in mesophilic and thermophilic conditions.
- The operating pressure and temperature of the inputs are atmospheric and ambient.
- The operating parameters of the reactors and reformers are taken from the literature and sensitivity analyses.
- AD and MEC biogas would feed both DBR and CBSR reformers.
- CO_2 capture by absorption process.
- Absence of deactivation during multiple desorption-reduction cycles.

The process simulation of hybrid AD and MEC coupled with DBR is shown in Fig. 2a. In the laid out system, the hydrolysis of AD digestate after mixing with H_2O feed produces acetic-acid ($C_2H_4O_2$) CO_2, xylose ($C_5H_{10}O_5$), furfural ($C_5H_4O_2$), CH_4, ammonia (NH_3), H_2S, arginine ($C_6H_{14}N_4O_2$), valine ($C_5H_{11}NO_2$), glycerol ($C_3H_8O_3$), tripalmitin ($C_{51}H_{98}O_6$) and others. The wastewater feed to MEC cools the synthesis gas exiting the DBR reformer and exchanges the absorbed heat with the hydrolysis product (thermal pretreatment). Acidogenesis enzymes in the CSTR accept the hydrolysis product (amino acids, glucose and long-chain fatty acids) and decompose into ethyl-cyanoacetate ($C_5H_7NO_2$), $C_2H_4O_2$, dioxolane ($C_3H_6O_2$), butene ($C_4H_8O_2$), CO_2, H_2O, NH_3 and others volatile fatty acids (VFAs) with total degradation reactions of 23. In the same CSTR, acetogenesis bacteria break down acidogenesis product into $C_5H_7NO_2$, $C_2H_4O_2$, $C_3H_6O_2$, H_2, CH_4, CO_2, H_2S and sulphur (S) in a total of 6 chemical reactions. The acetogenesis product flows to another CSTR (METH-GEN) to produce more CH_4 and CO_2 with reduced VFAs end-products. H_2, CO_2 and other by-products of acetogenesis are consumed by hydrogenotrophic methanogens microorganisms in the CSTR (METH-GEN). Aspen Plus unit operation model blocks and material streams description is given in Table 6 in the appendix. Unlike the AD process for CH_4 and CO_2 production, the MEC stack received cooled thermally treated wastewater and split it into CH_4 and CO_2 with the applied voltage <1V. Both by-products of AD and MEC mix in a mixer. The first separator and condenser allowed the exit of VFAs, sulphur and H_2O from the syngas.

Since this study focuses on the use of renewable energy sources, pressurised CH_4 and CO_2 by-products of AD and MEC flow from the first separator to the CSP furnace to absorb heat, and then to the reformer. The endothermic decomposition of CH_4 and CO_2 in the reformer produces synthetic gas (CO and H_2). The biosynthetic gas from the upstream reformer to the WGS transforms H_2O into steam in the heat exchanger. In WGS units, more H_2 is produced and CO is converted to CO_2 with the addition of steam from the heat exchanger. The produced biohydrogen is then separated from the CO_2 and stored. The CO_2 by-product was captured by reacting with calcium oxide (CaO) to form calcium carbonate ($CaCO_3$) for geological storage. Half of the steam produced by syngas cooling was utilised to drive the steam cycle to generate electricity. Calculator blocks with

Fortran codes were used to control pH value, temperature and feed rate. A small fraction of H_2 fuel was burnt in the reformer furnace to compensate for the heat loss between the solar parabolic dish (SPD) and the reformer. The integrated AD and MEC coupled with CBSR is shown in Fig. 2b. The integrated system follows the same operating procedure as Fig. 2a, except for the participation of the NiO catalyst in the reforming and the introduction of a cyclone for solid removal. A cyclone was used to ensure that the NiO catalyst was not carried to the shift reactors (WGS).

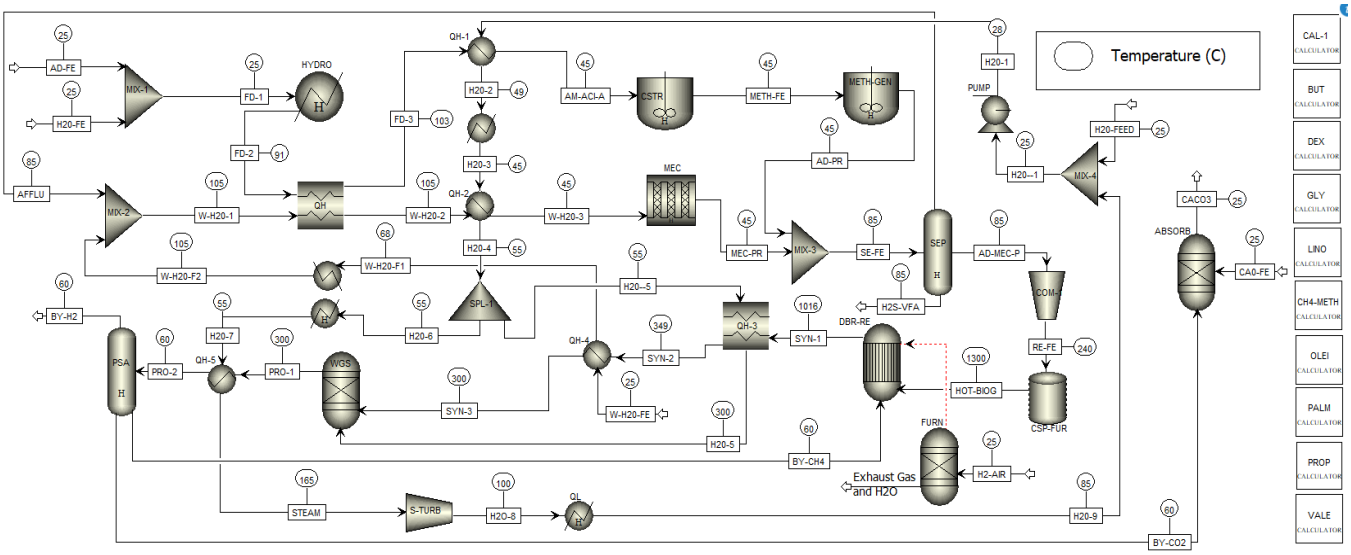

Fig 2a: ASPEN Plus flow diagram for integrated AD and MEC coupled with DBR.

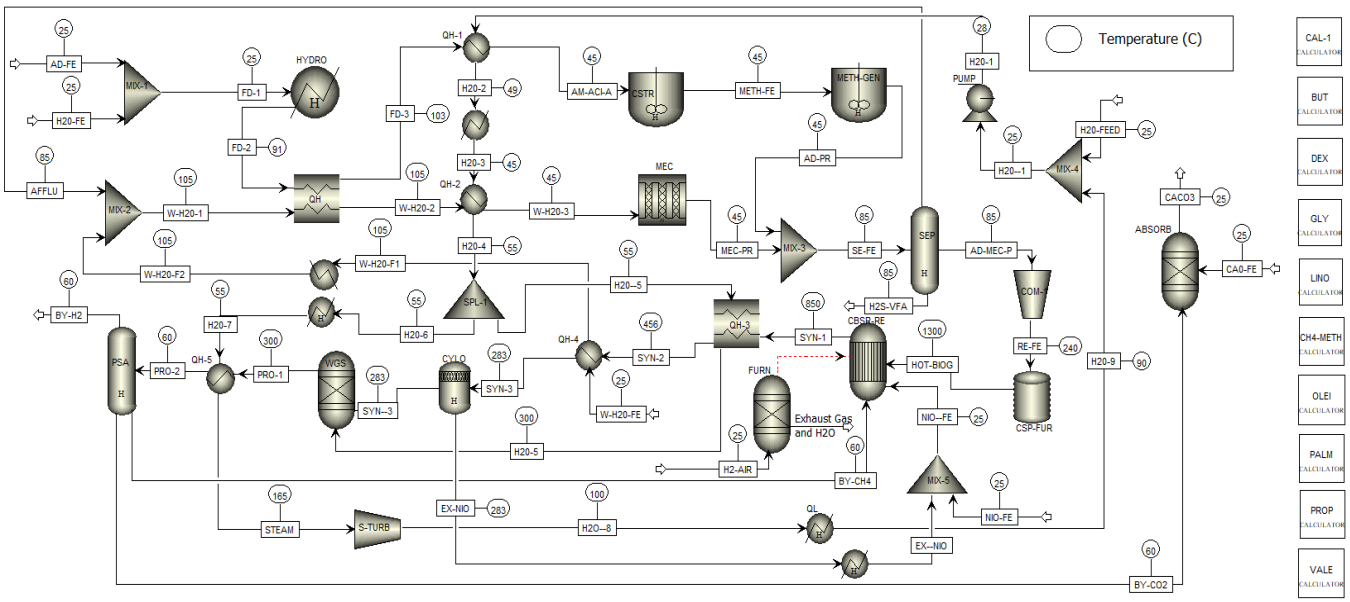

Fig 2b: ASPEN Plus flow diagram for integrated AD and MEC coupled with CBSR.

2.4 Computational models, meshing and boundary conditions of solar parabolic dish (SPD)

The SPD development employed Spalart-Allmaras (SA) with vorticity-based and corner correction options to simulate the conversion of photon energy to heat. These include the collection of solar radiation by the solar dish, the reflection of concentrated sunlight to the receiver furnace and the absorption of heat by the working fluid (CH_4 and CO_2). The solar radiation considered discrete ordinates with a computed sun direction vector at different irradiances (600, 650, 750, 950 and 1200W/m^2). Mesh independency was checked at different meshing types to maximise the fluid absorption efficiency. For 406710 cells, 10^{-6} convergence criterion equations for continuity, velocities and intensity were reached. The increase in element numbers for more cells gave nearly the same result. At this point, a meshed SPD with 406710 cells was adopted for the numerical investigation. Inlet, outlet, and wall are the three boundary conditions considered during the numerical study of the SPD unit. Aluminium for the solar dish and the working fluid penstock, and copper alloy for the solar thermal receiver were materials

utilised. The governing equations for continuity, energy and radiation intensity are given in Eqs 12 – 14. Fig. 3a displays the SPD unit for the heat source of the integrated system when the sun is available.

$$\frac{\partial}{\partial t} + \frac{\partial}{\partial x_i}(\rho u_i) = 0 \ (Continuity). \quad 12$$

$$\frac{\partial}{\partial t}(\rho_s c_s T_s) + \frac{\partial}{\partial x_i}\left[\lambda_s \frac{\partial T_s}{\partial x_i}\right] = 0 \ (Energy) \quad 13$$

$$U = \frac{W}{4\pi} \ (Radiation\ intensity) \quad 14$$

Where: ρ = mean density; u = velocity; λ = thermal conductivity; s = wall solid; T = operating temperature; W = power delivered to the solar receiver.

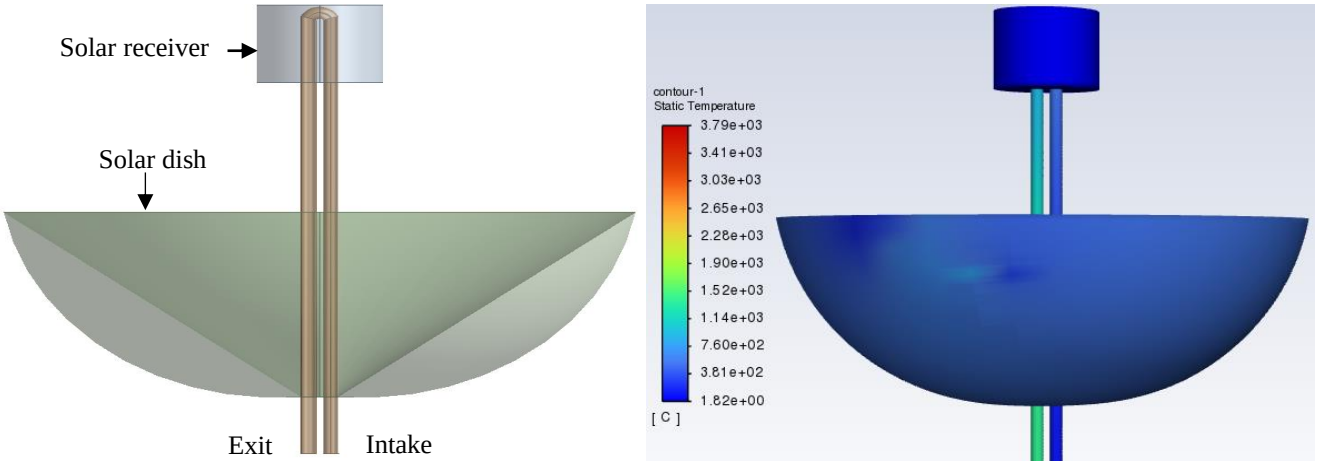

Fig 3a: Proposed solar parabolic dish (SPD) for reformers' heat source.

2.5 Solar and wind energy systems

Fig. 3b shows renewable solar and wind energy systems for the proposed system. A solar energy system generates electricity when photon energy reflects on the solar arrays containing p-type and n-type materials, causing the migration of electrons from donor to acceptor materials. The voltage and current blocks measure the output current and voltage of the solar array unit. The multiplier block calculates the total output electricity of the unit. 3kW of electrical energy was generated by the PV (Photovoltaic) system which is enough to operate the electrical units. The same power was produced by the wind turbine system. Since Aspen Plus is limited to the development of both solar and wind renewable energy systems for the electrical units of the hybrid system such as a MEC stack, the integrated AD and MEC coupled with CBSR was transformed into flow-driven for the Simulink interface. The integrated AD and MEC coupled with CBSR was considered over hybrid AD and MEC coupled with DBR due to the lower operating temperature (850°C) of the reformer. Fig. 4 shows an integrated AD, MEC and CBSR driven by SPD, solar cells and wind turbine energy systems. In the displayed hybrid system, the biogas (CH_4 and CO_2) from AD and MEC flows to the solar furnace of the SPD with an outlet temperature of 1300°C before endothermic decomposition in the CBSR reformer. While solar or wind power systems produce more electricity for MEC stack, pumps, compressors and separators depending on the sources available during operation. In the combined system, the working fluid is biogas (CH_4 and CO_2) and the heat output of the SPD is connected to the CSP furnace unit (CSP-FUR). While the electricity from any of the renewable sources (solar or wind) is connected to the electrical units to have the integrated system operate as a single unit.

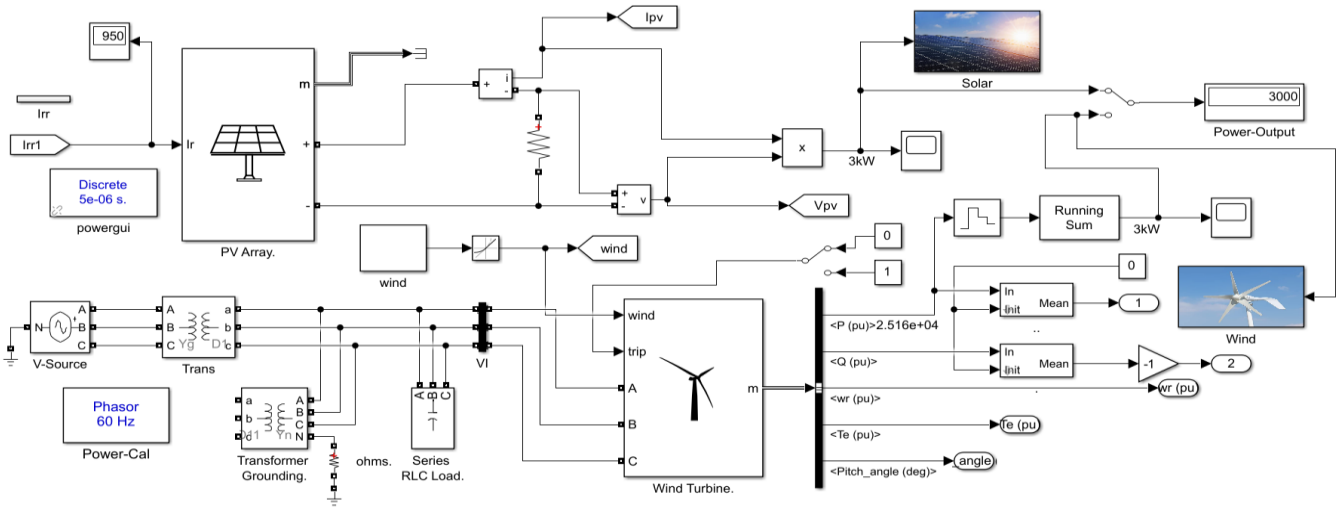

Fig 3b: Proposed solar cells and wind turbine system.

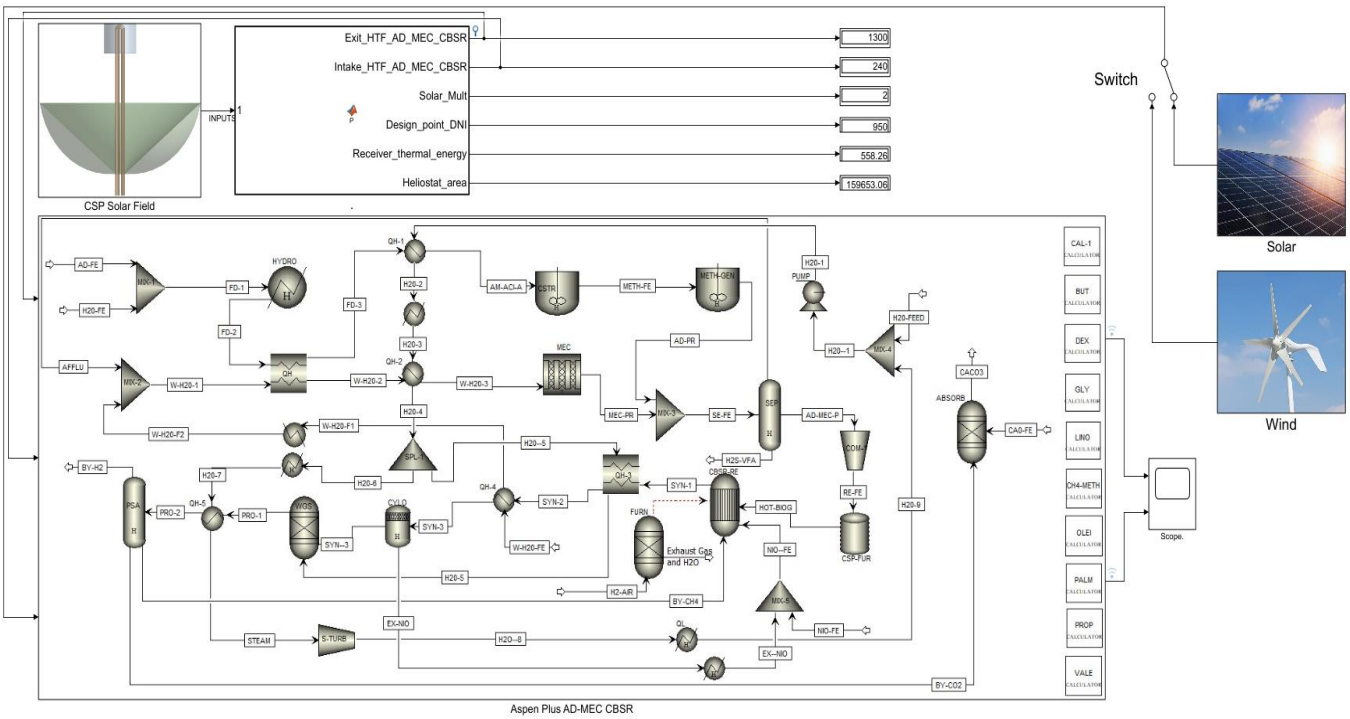

Fig 4: Flow diagram for integrated AD, MEC and CBSR driven by *SPD, solar cells and wind turbine energy systems.*

3. Results and Discussions

The inclusion of substrates pretreatment (thermal) was found to promote higher CH_4 and lower VFA productions. As reported by *Kondusamy & Kalamdhad.* [5], heat treatment of AD digestate between 160 and 180°C can increase CH_4 production by 20%. Instead, between 5 and 32% of biogas formation can be achieved at lower pretreatment temperatures. However, heat treatment below 160°C requires a longer duration. By pretreating the substrates with the recovered heat from the biogas reformer, the CH_4 formation rate increased by >5%. With the use of thermally pretreated feedstocks, an increase in microorganisms responsible for biogas production was seen. In addition, a reduced volatile solid (VS) content of 61% was observed in the AD unit by using pretreated feedstocks which also reduced the formation of hazardous substances such as H_2S and SO_2. The operating temperature of the digester is another important factor in the AD process, as it favours both VFA production and feedstock decomposition depending on the type of substrate. Mesophilic (35 - 40°C) and thermophilic (50 - 55°C) conditions are two favourable conditions for the development of AD microbes in the digester. As reported by *Holtzapple, et al.* [41], lower VFA production under thermophilic temperature conditions can be achieved in contrast to mesophilic conditions. Nonetheless, greater production of carboxylate salts is expected under thermophilic conditions. In this study, lower VFA and H_2S production was recorded under mesophilic and thermophilic conditions as *Rosa et al.* [42] mentioned that a

digester operating temperature between 25 and 60°C promotes microbes' activities, which increases biogas concentration. The pH value is another important factor in the AD process as an increase in VFA and H_2S formations is likely at a lower value (i.e. acidic conditions). For instance, *Vu et al.* [43] found that pH values between 7 and 8 can reduce the formation of SO_4^- and H_2S. In addition, a pH value <5 affects the H_2 concentration rate in the fermenter because of a declined hydrogenase (sporulating H_2-producing) microbes. A lower H_2 by-product in the acetogenic stages means a reduced CH_4 formation in the methanogenesis final stage as VFA combines with H_2 to form CH_4. Similar to the reduced H_2 concentration rate at lower pH values, a higher pH value (>8) is unfavourable for CH_4 production as methanogenesis enzymes will struggle to survive under such extreme conditions. Nonetheless, a pH value >8 favours H_2 concentration [44] [45]. Adjusting and manipulating pH value with chemicals like NaOH is an effective way to arrest methanogenesis. In this study, equilibrium digester OLR to prevent overloading improved enzymes' decomposition activities. OLR and other parameters like pH, temperature HRT were controlled using calculator blocks with Fortran codes. The results show that adjusting the mesophilic and thermophilic temperature conditions, pH value and feed rate of the digester in a process simulation is possible and reliable because the program allows proper conditioning of each of these parameters of AD reactors. The results of integrated AD and MEC coupled with DBR and CBSR processes for H_2 generation are given in Table 3. By adding a second CSTR for methanogenic bacteria with minimal stirring, 0.062% of CH_4 formation was observed. This is very important to improve the purity of AD and MEC biogas. Higher CH_4 formation in the first stage digester indicates the presence of methanogenic microbes. In contrast, lower CO_2 production was observed in the methanogenic digester. As recorded in the result Table, CH_4 production by hybrid AD and MEC outperforms conventional AD and MEC as proposed by many researchers. For example, recent reviewers have suggested adding cathode and anode electrodes to the AD fermenter to improve overall efficiency. Heat treatment of AD digester to increase biogas production was also found to be energy intensive in a single unit without waste heat recovery and utilisation, despite the reduction of VFA. In this study, the efficiency of the AD unit reached >67%, which is almost the same as the efficiency of another AD unit reported in the literature with pretreated substrates [46]. While the MEC unit of this study achieved an efficiency of ≥64% which is similar to that reported in the literature. For example, using a spent dark fermentation (DF) for MEC substrate, an efficiency of 64% was reported [47] [48] [49]. In contrast to the MEC with noble metal-catalysed electrodes, a lower efficiency was seen in this study as *Kadier et al.* reported a MEC efficiency of 69% [50]. The higher efficiency of both AD and MEC units of this study was also facilitated by using a mixed-culture MEC as dual-chamber MEC uses a proton exchange membrane (PEM) stack which increases energy input. For instance, preventing gas cross-over in a dual electrolyser system by using a membrane separator, requires more energy input in contrast to an industrial gas separation system [51].

Not long ago, a few studies showed the importance of dry reforming (DR) for H_2 production using biogas from AD or MEC due to the high cost of biogas membrane separators and energy loss due to polarisation resistance. However, the results of this study show that catalytic biogas reforming with NiO as a reforming catalyst is less energy-intensive and requires half the mass flowrate of fuel combustion in the reformer furnace to compensate for the heat loss. For example, the simulation of the dry biogas reforming (DBR) process displayed in Fig. 2a shows that an optimal reaction temperature of about 1000°C is required to convert AD and MEC by-products (CH_4 & CO_2) to CO and H_2 before the application of WGS units. In contrast, CH_4 and CO_2 reached the highest conversion rates at the catalytic biogas steam reforming (CBSR) reaction temperature of 850°C. The application of CO_2 by-product capture by absorption process shows that more thermal energy can be recovered because the reaction of CaO and CO_2 to form $CaCO_3$ is exothermic. Furthermore, the application of the steam cycle allowed waste heat to electricity conversion in addition to renewable solar and wind energy systems for electrical equipment. A small fraction of produced H_2 was burnt in the reformer furnace to make up for losses between the SPD and the reformer. This approach of using renewable electricity and low-carbon fuel eliminates the burning of fossil fuels in the reformer furnace and the dependency on grid electricity. By using Eq 15 which is an equation for estimating the efficiency of the system, an efficiency of 66% was recorded which is similar to the literature reported plasma-assisted DR efficiency [52]. The thermal efficiency of the solar thermal unit reached 60%. The mean (average) efficiency of the proposed system without solar and wind power systems is approximately 64%. For renewable power systems, the estimated efficiencies were ≤45% for a wind turbine and ≤20% for solar cells.

$$Efficiency\ (n) = \frac{H_2\ LHV * mass\ flowrate\ of\ produced\ H_2}{Energy\ input} \quad 15$$

Thus, the proposed simulated systems have shown that biohydrogen production without a carbon footprint and minimal exergy loss is possible by using biomass, organic waste, wastewater and steam as feedstocks. By using organic young plants and other biomass feedstocks and replanting used feedstocks, about 10.92kg of atmospheric CO_2 for 1kg of H_2 can be captured as plants fix CO_2 from the atmosphere during photosynthesis and store it in their roots. This is feasible because the solar thermal system produced the required heat, solar or wind power systems generated electricity for the electrical units, oxy-hydrogen to compensate for the loss heat and by-product CO_2 from the process was captured. However, considering the life cycle analysis of the entire system, $1kg_{H_2}$ may remove <10.92kg of atmospheric CO_2.

Table 3: Feed and product results of integrated AD and MEC, coupled with DBR and CBSR.

Streams	AD		MEC		DBR		CBSR	
	Feed	Product	Feed	Product	Feed	Product	Feed	Product
Digestate & Wastewater $(kmol)$ (kg)	0.94 149.13		18 576.50					
H_2O $(kmol)$ (kg)	2.4	1.27		12	17.43		17.43	
CH_4 $(kmol)$ (kg)		3.1 48.99		6 96.26	9.1 145.25		9.1 145.25	
CO_2 $(kmol)$ (kg)		2.7 119.39		6 264.10	8.7 382.89	17.43 767.10	8.7 382.89	17.43 767.10
NH_3 $(kmol)$ (kg)		0.00001						
H_2S $(kmol)$ (kg)		0.003 0.1						
VFA & others $(kmol)$ (kg)		0.0001						
H_2 $(kmol)$ (kg)		0.0005				34.85 70.26		34.85 70.26
S $(kmol)$ (kg)		0.00002						
NiO $(kmol)$ (kg)							17.43 1301.51	
CaO $(kmol)$ (kg)					17.43 977.18		17.43 977.18	
$CaCO_3$ $(kmol/hr)$ (kg/hr)						17.43 1744.10		17.43 1744.10

3.1 Model validation and comparison.

The validation of the simulated AD method for biomethane production was carried out part by part. Unlike *Hajizadeh et al* [7] study, the simulated model achieved lower NH_3, H_2S and VFAs values because thermal substrate pretreatment aided the reduction of total solid (TS). In addition, lower production of acid-like by-products was also possible by using a second digester for methanogenic bacteria in conjunction with heat pretreatment of the complex digestates. For instance, *Guo et al*. [53] found that the yield of biohydrogen and biomethane depends on the reactor configuration, the pretreatment method, the type of substrate used, and the digester temperature. Variation in the carbohydrate composition of biogas substrates means that carbohydrate-rich feed has high syngas concentration during AD or dark fermentation (DF) [53]. With the use of carbohydrate-rich substrates, more biogas yield is expected. The minimal production of other forms of VFA means that a higher biogas conversion rate was achieved in this study compared to *Hajizadeh et al*. [7] investigation. Comparing the AD unit of this study against *Wang et al.* [54] work, both are in agreement with minimal difference. For example, using food waste (FW) and garden waste (GW) or kitchen waste (KW) as substrate at a ratio of 80:20 and 60:40 without pretreatment, an efficiency of 61.91% was reached [54]. The use of thermally pretreated substrates promoted a higher AD efficiency (64%) in this study, in contrast to the *Hajizadeh et al* study.

Comparing the reported MEC efficiency of *Kundu et al.* [49] work to this study, a minimal difference was attained. *Kundu et al.* studies include the use of precious metal for the configuration of MEC at an applied voltage of 0.8V. Such MEC stack configuration facilitated higher exoelectrogens' activities but also increased the cost of the H_2 sales price. Validating the reforming units of this developed system with *Su et al.* [23], lower exergy loss was achieved by using a solar thermal source to

produce about 95% of the required heat and burning a small fraction of H_2 fuel to meet the reformer heat demand. Exergy destruction of this system was <20% compared to 44.08% for SMR and 34.03 % for DR in *Su et al.* [23] investigated work. Contrasting the solar receiver thermal efficiency of SPD of this system with *Castellanos et al.* [32], both studies achieved nearly the same result. For example, solar dish thermal efficiency of 86% was reported by *Castellanos, et al.* [32]. In this study, a receiver efficiency of 86% was observed at higher solar radiation. However, the efficiency of the receiver can be increased to 90% by integrating a solar tracking system and using a material that increases the heat reflection from the solar dish to the receiver furnace under higher solar radiation. The overall efficiency of the solar thermal unit (60%) in this study agrees with that reported by *Subramani et al*. [55]. For example, a solar parabolic dish collector (SPDC) efficiency between 45% and 62% was recorded by *Subramani et al*. during SPDC analysis for rural heating systems. Fig. 5 shows a comparison of this study with the related studies in reference to the efficiency of each unit. Table 4 illustrates the model validation against similar studies, while Table 5 compares this work to other biohydrogen, green and blue H_2 production processes.

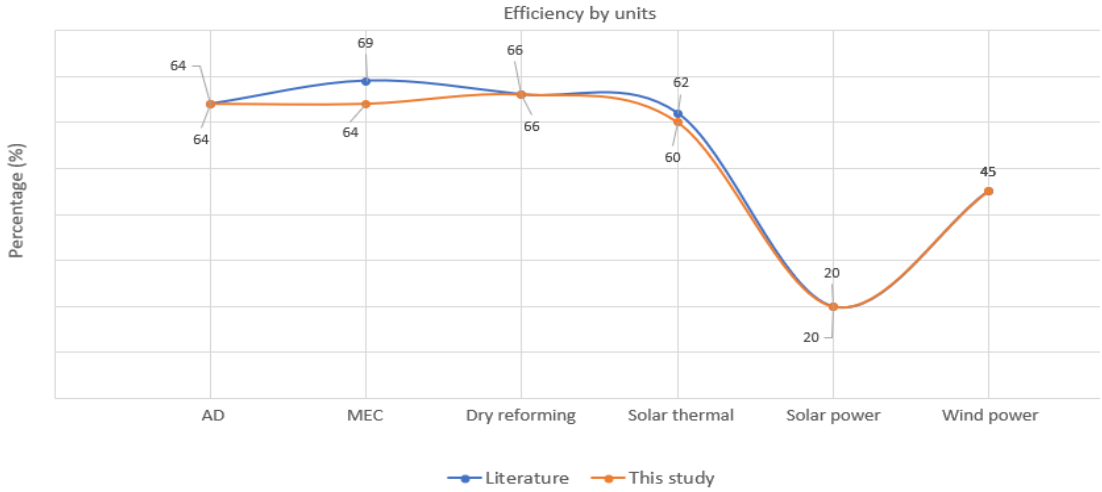

Fig 5: Comparison of this work with the related studies based on efficiency [47] [48] [49] [50] [52] [55] [56] [57].

Table 4: Model validation against literature data on AD unit [58].

Component	This study (volume %)	Agricultural (volume %)	Waste (volume %)	Landfill (volume %)
CH_4	44	49 – 69	44 – 67	40 – 70
CO_2	38	29 – 44	30 – 44	25 – 40

Table 5: Comparison of the developed system with other H_2 production process [59] [60] [61] [62] [63].

H_2 production technologies	Substrates (Feedstocks)	Form of energy for operation	Efficiency (%)	Advantages	Drawbacks	Cost ($1kg_{H_2}$)
Electrolysis of H_2O	H_2O	Electricity Heat for distillation or steam production.	59 - 100	Renewable source.	Required distilled H_2O feedstock. Energy intensive.	\$5 – \$10/kg_{H_2}
Thermolysis	H_2O H_2SO_4	Electricity Heat	>59	Lower stack operating temperature. Renewable source.	Sulphur poisoning of membrane. Energy intensive.	Cheaper than H_2 from H_2O electrolysis.
Photolysis	H_2O	Photon Electricity	30	Renewable source.	Corrosion. Instability. Low efficiency.	\$3.12/kg_{H_2}
Bio-photolysis	H_2O	Photon or light	<2	Renewable source.	O_2 sensitive.	\$1.42 – \$7.44/kg_{H_2}

					O_2 cross-over to H_2ase microbes' chamber. Low efficiency.	
Bio-electrochemical	Organic waste Acidified H_2O or wastewater Salt-solution H_2O	Electricity	41 - 75	Waste to energy. Renewable source.	High cost of membrane separator. Energy intensive.	\$6/kg_{H_2}
Fermentation	Organic waste	Photon or light for photo-fermentation Electricity	25 - 70	Waste to energy. Renewable source.	High VFA by-product. Low H_2 yield.	\$2.3 - \$7.61/kg_{H_2}
Hydrocarbon reforming with CCS, including dry reforming	Fossil fuels H_2O	Heat Electricity	60 - 85	High efficiency. Cheaper H_2 sales price.	Carbon emissions. Non-renewable feedstock.	\$2 - \$3/kg_{H_2}
This study	Organic waste Biomass Wastewater H_2O	Electricity Heat	≥64	Waste to energy. renewable source. Solar thermal for heat production. High biogas yield. Low VFA production.	VFA by-product. Less efficient in cold regions because photon energy is required to produce heat.	\$2 - \$6/kg_{H_2}

3.2 Sensitivity analyses on OLR, HRT, temperature, pressure, and solar irradiance effect on syngas production.

The importance of other parameters such as pH was highlighted, but organic loading rate (OLR) and hydraulic retention time (HRT) are other factors that affect the biogas production in the AD method. For instance, *Kang et al.* [64] studies on the effect of OLR found a daily bigas (H_2) formation of 0.06, 0.08 and 0.11l at a loading rate of 3 days intervals. An increase in biogas formation was also observed at higher feed rates, which contradicts *Hajizadeh et al.* [7] results. A decrease in syngas formation (CH_4) due to an increase in OLR was reported by *Hajizadeh et al.* [7]. Fig. 6 shows the effect of different OLR and HRT on biogas formation. From the analysis result, the biogas from the AD fermenter decreases as the feed rate increases until the CSTR volume is filled. The slow activity of the enzyme responsible for biogas production was attributed to the decrease in biomethane production caused by the feed rate increase. In contrast, the volume of biogas concentration increases by increasing the HRT. The results of sensitivity analyses on the effect of OLR and HRT on biogas production agree with *Hajizadeh et al* and *Liu, et al.* [65] findings. Nevertheless, by increasing OLR and using a larger digester volume, biogas production is expected to increase after a few days, as a larger reactor volume will enable microorganisms access to the available substrates.

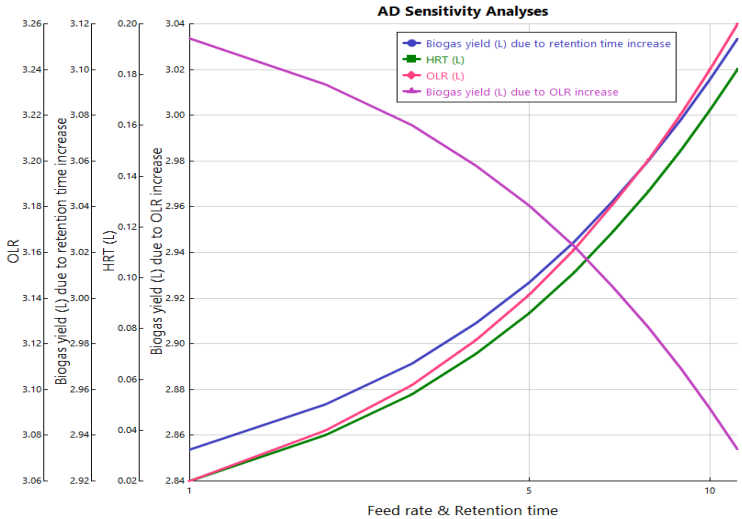

Fig 6: Effects of different OLR and HRT on biogas formation

Similar to HRT in biogas production, catalytic syngas decomposition in the reformer is dictated by the influence of temperature and pressure. As displayed in Fig. 7a and 7b, reaction pressure and temperature between 1 and 25 bar and from 100°C - 1000°C were utilised during temperature and pressure analyses on syngas production. At temperature <400°C, the syngas production rate was relatively low due to the endothermic nature of both dry and catalytic reforming systems. Syngas formation increases as the reaction temperature increases which is opposite to the pressure increase. The operating temperature of dry biogas reforming (DBR) was kept at 1000°C to achieve complete conversion (about 99%) of the feedstock. Unlike DBR, catalytic biogas-steam reforming (CBSR) achieved 99% feed decomposition at a reaction temperature of 850°C. Temperature and pressure analyses show that syngas formation under endothermic conditions is favourable to optimum reaction temperature. The operating pressure of both integrated systems was kept at 4 bar because the increase in pressure increases syngas purity but requires more thermal energy input to achieve a complete decomposition. Increasing the operating pressure without increasing the reaction temperature decreases the syngas conversion rate due to the endothermic nature of the feedstock. *Shehzad et al.* [66] reported a similar result on the effect of temperature and pressure on syngas formation.

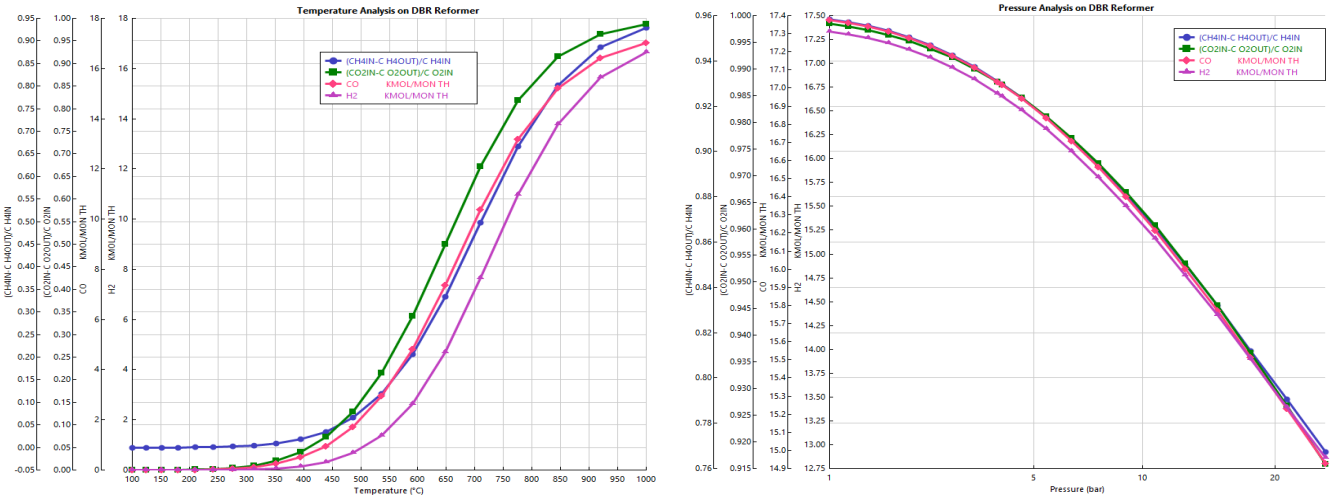

Fig 7a: Temperature and pressure effect on syngas production on DBR process of hydrogen production.

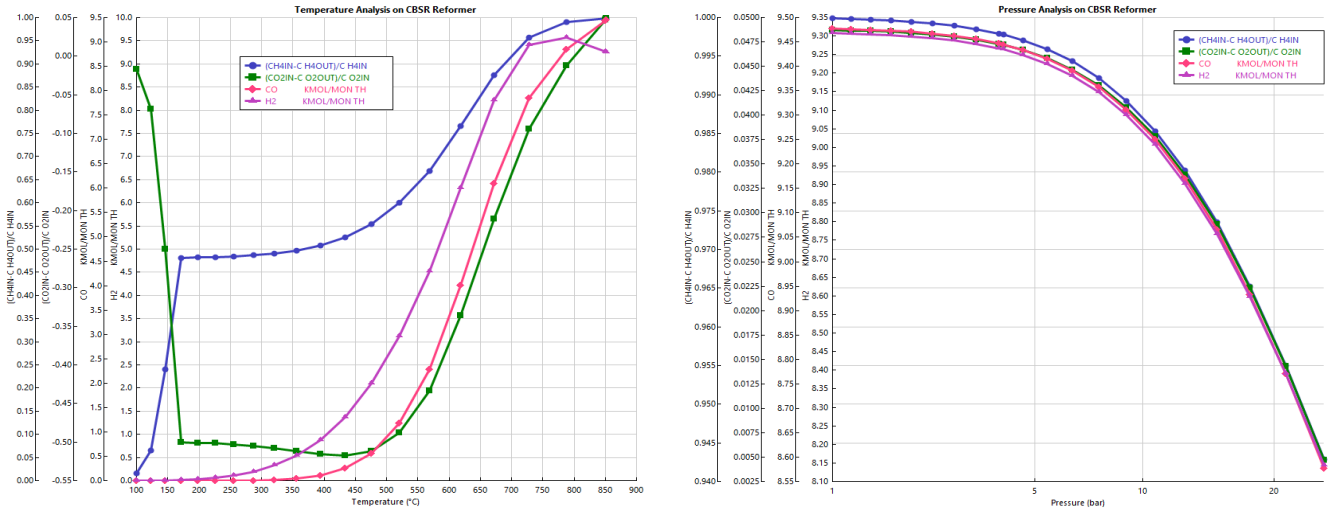

Fig 7b: Temperature and pressure effect on syngas production on CBSR process of hydrogen production.

Fig. 8 represents the effects of solar irradiation intensity on the exit temperature of the working fluids to the reformer. As the solar irradiance reflecting on the dish increases, the temperature of the exit working fluid increases. This shows that the amount of photon energy converted to heat increases as the irradiance rises. The temperature of the working fluids (CH_4 and CO_2) as the solar irradiation intensity increases or decreases is the only factor that changes over time. A similar result was reported from the literature on a photovoltaic/solar thermal (PV/ST) collector with H_2O as the only working fluid [67].

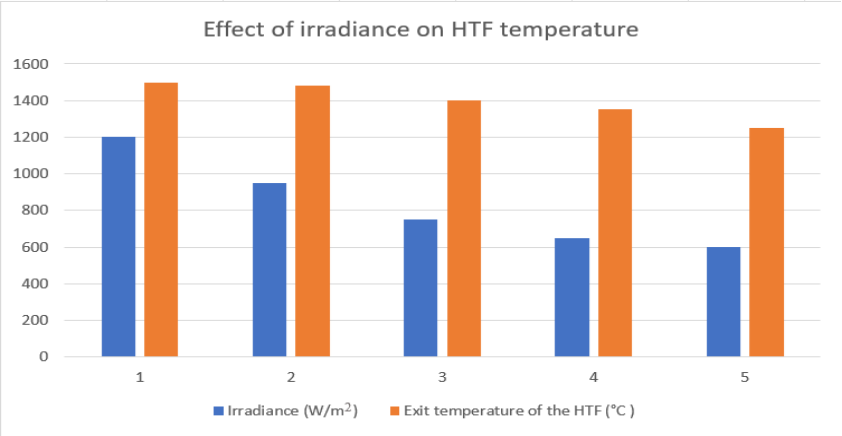

Fig 8: Effect of irradiance on HTF temperature.

3.3 Energy analysis

Various pretreatment methods for AD digestate have been developed by many researchers to maximise syngas formation and reduce VFA production. Some of the pretreatment methods like steam explosion and $Ca(OH)_2$ increased the efficiency of biogas production by 61.54% [68]. For this reason, a combined steam explosion and $Ca(OH)_2$ at a higher operating temperature (250°C) and pressure (15 bar) was proposed for digestates pretreatment to promote syngas conversion efficiency and reduce the pretreatment length in biogas production systems [69]. However, the thermal and high-pressure feedstocks' pretreatment of biogas production systems increases operation and maintenance costs. By incorporating SPD and heat recovery units for AD and MEC digestates' pretreatment and steam production, this developed system mitigates high-temperature pretreatment costs and reduces the operation time to one week. Unlike photo or dark fermentation, aerobic or anaerobic digestion and dual-chamber MEC pathway of biohydrogen production, producing biogas from both AD and mixed-culture MEC units and converting the produced biogas to biohydrogen through dry or catalytic reforming are less energy intensive and more efficient. With this proposed system, the need for external heat for substrates pretreatment and more power input to electrolyser stack because of resistivity caused by the presence of membrane separator, were avoided. This developed system can still accommodate natural gas or CH_4 feedstock to increase the H_2 production rate, which other biohydrogen production methods lack. In addition, waste heat to electricity via a steam cycle means that more energy can be stored when this developed system is in operation to operate the AD unit in the absence of sun or wind. In this proposed system, $<4kg_{CO_2}/kg_{H_2}$ was obtained and captured by using SPD and oxy-hydrogen combustion for endothermic decomposition of the biogas in both reformers. In addition, between 0.1 and $4.35kgCO_2/m^3$ was prevented in biogas production units (AD and MEC) by using solar or wind energy systems for the operation of the electrical units and recovered heat for the pretreatment of the digestate. For example, hydrocarbon reforming methods such as SMR (steam methane reforming) without carbon capture and storage (CCS) units emit $13.7kg_{CO_2}$ for every $1kg_{H_2}$ by-product [59].

3.4 Economic analysis

The predominant activated sludge (AS) route for wastewater and organic waste treatment plants relied on heterotrophic microbes that consume organic compounds or substances using an O_2 electron acceptor and release CO_2 in the process. Due to the energy intensive of the AS tank (≥60%), AD and MEC pathways in contrast to aerobic and fermentation routes were proposed to recover energy such as H_2 instead of consuming it. The introduction of these systems in waste treatment sectors can minimise plants' size and operation costs [70]. However, low chemical energy (H_2) recovery and higher energy demand and cost because of internal resistance caused by the presence of membrane electrodes and a separator led to the transition to AD and mixed-MEC with pretreated substrates. For example, between \$1,237 and \$3,263/m^3 was the estimated cost of the membrane electrode compartment including the separator, leading to further research into the use of transitional metals like stainless steel and carbon nanocomposite for mixed culture MEC [71] [72] [73]. At a material cost of \$6.32 –12.64/m^2_{anode}, MEC for wastewater treatment would be financially competitive [74]. In addition, *Krishnan et al.* mentioned that the reduction of electrolyser stack costs from \$422 to \$85.92/kW and from \$1,164.86 to \$254.49kW by 2030 is feasible [75]. Achieving

waste-to-energy sustainability in waste treatment plants requires lower production and operation costs, the use of transition metals for anode and cathode electrodes and methanogenic pathways to promote higher conversion of VFA to biogas. In addition, AD power plants with a capacity of 100kW - 1000kW can experience a payback period of 4 - 5 years at a localised electricity cost of \$0.55/kWh. An installed AD plant with a capacity of 1 tonne costs \$618 for investment and \$53 for operation. In theory, a tonne of organic waste such as food waste can produce 247m^3 which can generate 90GJ of heat (847kWh electricity) [76] [77] [78] [79]. Furthermore, at daily production of 379,387kg_{H_2} from hydrocarbon reforming (SMR), feedstock cost accounts for 61%, 29% goes for investment and the remaining 10% for both operation and maintenance (O&M) at a sales price of <\$2.5kg_{H_2} [80]. As H_2 purchase price from dual-chamber MEC is not more than \$6/kg_{H_2}, and both cheaper and sustainable means of H_2 production have been demonstrated, this developed system put the produced H_2 sales price between 2/kg_{H_2} and \$6kg_{H_2}.

A higher H_2 sales price of this system in contrast to biomass pyrolysis and integrated AD-DR is attributed to the presence of a MEC unit and renewable energy systems. For example, *Parkinson et al.* [81] reported a H_2 selling price from \$1.18/kg to \$1.89/kg for pyrolysis of CH_4. On the contrary, the studied CH_4 pyrolysis system excluded a CCS unit and the reported H_2 cost came from the pyrolysis unit operating with a fossil fuels' decomposer furnace. Furthermore, *Hajizadeh et al.* [7] studied work on hybrid AD-MEC with a H_2 purchase price of \$1.39/kg avoided CO_2 by-product capture and the use of renewable energy sources for system operation. Besides, the reported efficiency (73%) and H_2 sales price by *Hajizadeh et al.* were based on theoretical assumption and questionable because the studied work used unpretreated substrate that increases TS and VFA contents and the DR efficiency is <67%. In addition, a cheaper H_2 selling price is possible by increasing the production rate of biogas from the AD and MEC units and H_2 from either a DBR or CBSR as *da Silva et al.* [82] reported a sales price of 2.54/kg_{H_2} for integrated biogas reforming and fuel cell system. Furthermore, a H_2 sales price for both integrated systems is expected to decrease further when installed in MENA (Middle East and North Africa) countries. For instance, *Lilliestam & Pitz-Paal.* [83] reported an electricity price of \$0.07/kWh for CSP systems operating in Dubai (DEWA IV) which is below \$0.14/kWh for another CSP operating in China [84]. Although, *Singh et al.* [85] analysis of seasonal variations in solar energy concluded that the absence of dust on reflective surfaces such as a solar dish or heliostats due to continuous rain increases absorption efficiency despite higher solar irradiation in the summer season.

3.5 Environmental assessment

The transition to renewable sources of heat and electricity is encouraged to limit the temperature rise above 1.5°C by 2030. In addition, the recovery of biogas from organic and other waste matters will play an important role in reducing GHG emissions by 2030. However, challenges related to AD end-use management and operations in developing countries must be addressed for waste or biomass to low-carbon fuel. For example, the lack of appropriate technologies, operators, markets for end-use and waste management in developing countries like India has hindered the growth of the AD system [86].

The simulated renewable aided biomethane and biohydrogen productions with a carbon capture unit can replace direct air capture (DAC) technologies that remove CO_2 directly from the atmosphere. For example, the use of organic wastes and biomass (young plants) as feedstocks means that CO_2 captured by plants during photosynthesis can be stored underground as plants use CO_2 to produce glucose during photosynthesis and store it in their roots. However, this study also recommends replanting when biomass feeds such as agricultural products or plants are used. For example, using agricultural products such as maize silage will yield more biogas, but have environmental impacts without replanting. Substitution of biomass feeds for animal slurry will also affect marine and terrestrial ecotoxicity. Therefore, this study encourages the use of slurry and waste in a small-scale unit instead of large-scale systems utilising agricultural products as substrates.

Conclusion

To improve the efficiency of biohydrogen production in a cleaner way, solar and wind aided AD and MEC systems were developed and simulated. Pretreatment of AD and MEC feedstocks using the recovered waste heat, controlled pH value, OLR and HRT improves biogas formation by >5%. The inclusion of both DBR and CBSR processes in AD and MEC allowed the addition of WGS to increase biohydrogen production rate and convert CO to CO_2. Biomethane production in acidogenic and acetogenic fermenters indicates the presence of methanogenic microorganisms in the fermenter. A decrease in daily biomethane

production due to an increase in the feed rate was observed. Equilibrium OLR and the use of larger reactor volumes are necessary to improve biomethane production. The developed model achieved a price range of $2/kg_{H_2}$ - $\$6 kg_{H_2}$ and further H_2 purchase price reduction by increasing the production rate and deploying the hybrid system in areas with higher solar irradiation and longer sunny days is expected. Carbon emission from the process was avoided by using a CSP unit for heat production, recovered heat for feedstocks' pretreatment, solar cells and a wind turbine energy system for electricity generation and by-product CO_2 capture by absorption. A reduced exit temperature of the CSP heat transfer fluid (HTF) was observed at lower solar irradiance. Sensitivity analyses show that lower operating pressure and higher operating temperature favour biogas production in the reformer. An efficiency of 64% was achieved with lower VFA formation. Further studies should consider the use of DF by-products such as VFA as an AD substrate to maximise its (DF) efficiency. The simulated innovative models recommend a pilot-scale development for a sustainable H_2 economy.

Declaration of Competing Interest

The authors declare that they have no known competing financial interests or personal relationships that could have appeared to influence the work reported in this paper.

Appendix

Table 6: List of Aspen Plus unit operation model blocks and material streams description.

Aspen Plus Block Name	Aspen Plus Block ID	Description
Mixer	MIX	Mixing anaerobic digestion feed with H_2O. Merge 2 streams.
Splitter	SPLI	Split a stream into two or more streams. Split H_2O stream into 2 for WGS and S-turbine (steam turbine).
Hierarchy	HYDRO/METH-GE/CSTR	Container for directories. Act as a subsystem having a set of blocks that are grouped into a single hierarchy block. Has an icon of H. House RGibbs for electrochemical separation of wastewater into CH_4 and CO_2 with an ID name "MEC". House CSTR.
Heat exchanger	QH	Transfers heat from one medium to another. For thermal pretreatment of AD and MEC feeds. For generating steam for WGS and steam turbine.
Cooler	QL	Thermal and phase state changer. For feed or product cooling.
Rigorous continuous stirred tank reactor	RCSTR	Rate-controlled reactions based on known kinetic. For acidogenesis, acetogenesis and methanogenesis reactions model.
Separator	PSA/SEP	Split/separate products based on specified flows/fractions. Separate H_2 gas from others.
Rigorous reactor (RGibbs)	DBR-RE/ CBSR-RE/ WGS/ABSORB	Set the composition of product/syngas by chemical equilibrium restriction. Gibbs free energy reactor. To produce H_2 and CO. For H_2 and CO_2 production.
Turbine	S-TURB	For electricity generation. Calculate pressure drop after work is done.
Compressor	COM	Increase feed pressure to the desired level. Manly effective in the gas phase.
Pump	PUMB	Increase feed pressure to the desired level. More effective in the liquid phase.
Aspen Plus stream ID		Description
FE		Feed.
AD-FE		Anaerobic digestion feed, mostly organic waste/biomass.
W-H_2O-FE		Wastewater feed to MEC.

H_2O/any stream that starts with H_2O	Water (H_2O) stream.
FD/any stream that starts with FD	Digestate feed before and after hydrolysis.
PRO/any stream that starts with PRO	Product/syngas to the PSA (pressure swing adsorption) separator after decomposition.
SE-FE	A mixture of AD and MEC by-products to the separator.
AD-MEC-P	Syngas by-product of AD and MEC.
HOT-BIOG	Syngas by-product of AD and MEC leaving CSP furnace to DBR/CBSR reformers.
BY-H_2	Hydrogen (H_2) by-product.
BY-CO_2	Carbon dioxide (CO_2) by-product.
BY-H_2O	Water (H_2O) by-product.
BY-CH_4	Methane (CH_4) by-product.
SYN/any stream that starts with SYN	Syngas

Reference

[1] Magnuson, A., Mamedov, F., Messinger, J. (2020). Toward Sustainable H_2 Production: Linking Hydrogenase with Photosynthesis. *Joule, 4*(16), pp. 1157 - 1159.

[2] Rajendran, K., Kankanala, H. R., Lundin, M., Taherzadeh, M. J. (2014). A novel process simulation model (PSM) for anaerobic digestion using Aspen Plus. *Bioresource Technology, 168*, pp. 7 - 13.

[3] Thanarasu, A., Periyasamy, K., Subramanian, S. (2022). An integrated anaerobic digestion and microbial electrolysis system for the enhancement of methane production from organic waste: Fundamentals, innovative design and scale-up deliberation. *Chemosphere, 287*(1), p. 131886.

[4] Wang, W., Lee, D. J. (2021). Direct interspecies electron transfer mechanism in enhanced methanogenesis: A mini-review. *Bioresource Technology, 330*, p. 124980.

[5] Kondusamy, D., Kalamdhad, A. S. (2014). Pre-treatment and anaerobic digestion of food waste for high rate methane production – A review. *Journal of Environmental Chemical Engineering, 2*(3), pp. 1821 - 1830.

[6] Zhang, R., Zhang, M., Mou, H., An, Z., Fu, H., Su, X., . . . Sun, F. (2023). Comparation of mesophilic and thermophilic anaerobic co-digestion of food waste and waste activated sludge driven by biochar derived from kitchen waste. *Journal of Cleaner Production, 402*, p. 137123.

[7] Hajizadeh, A., Mohamadi-Baghmolaei, M., Saady, N. M., Zendehboudi, S. (2022). Hydrogen production from biomass through integration of anaerobic. *Applied Energy, 309*, p. 118442.

[8] Aramrueang, N., Rapport, J., Zhang, R. (2016). Effects of hydraulic retention time and organic loading rate on performance and stability of anaerobic digestion of Spirulina platensis. *Biosystems Engineering, 147*, pp. 174 - 182.

[9] Jain, S., Jain, S., Wolf, I. T., Lee, J., Tong, Y. W. (2015). A comprehensive review on operating parameters and different pretreatment methodologies for anaerobic digestion of municipal solid waste. *Renewable and Sustainable Energy Reviews, 52*, pp. 142 - 154.

[10] Liang, D., Zhang, L., He, W., Li, C., Liu, J., Liu, S., . . . Feng, Y. (2020). Efficient hydrogen recovery with CoP-NF as cathode in microbial electrolysis cells. *Applied Energy, 264*, p. 114700.

[11] Noori, M., Ghangrekar, M., Mukherjee, C., Min, B. (2019). Biofouling effects on the performance of microbial fuel cells and recent advances in biotechnological and chemical strategies for mitigation. *Biotechnology Advances, 37*(8), p. 107420.

[12] Nguyen, H. T., Noori, M. T., Min, B. (2022). Accelerating anaerobic digestion process with novel single chamber microbial electrochemical systems with baffle. *Bioresource Technology, 359*, p. 127474.

[13] Anukam, A., Mohammadi, A., Naqvi, M., Granström, K. (2019). A Review of the Chemistry of Anaerobic Digestion: Methods of Accelerating and Optimizing Process Efficiency. *Processes, 7*(8), p. 504.

[14] Lee, M. E., Ahn, Y., Shin, S. G., Chung, J. W. (2022). Enhancement of Biogas Production in Anaerobic Digestion Using Microbial Electrolysis Cell Seed Sludge. *Energies, 5*(19), p. 7042.

[15] Nguyen, V. K., Chaudhary, D. K., Dahal, R. H., Trinh, N. H., Kim, J., Chang, S. W., . . . Nguyen, D. D. (2021). Review on pretreatment techniques to improve anaerobic digestion of sewage sludge. *Fuel, 286*, p. 119105.

[16] Ismail, A., Kakar, F. l., Elbeshbishy, E., Nakhla, G. (2022). Combined thermal hydrolysis pretreatment and anaerobic co-digestion of waste activated sludge and food waste. *Renewable Energy, 195*, pp. 528 - 539.

[17] Climent, M., Ferrer, I., Baeza, M. d., Artola, A., Vázquez, F., Font, X. (2007). Effects of thermal and mechanical pretreatments of secondary sludge on biogas production under thermophilic conditions. *Chemical Engineering Journal, 133*(1 - 3), pp 335 - 342.

[18] Carrère, H., Bougrier, C., Castets, D., Delgenès, J. P. (2008). Impact of initial biodegradability on sludge anaerobic digestion enhancement by thermal pretreatment. *Journal of Environmental Science and Health, Part A, 43*(13), pp. 1551 - 1555.

[19] Wang, W., Lee, D. J., Lei, Z. (2022). Integrating anaerobic digestion with microbial electrolysis cell for performance enhancement: A review. *Bioresource Technology, 244*(B), p. 126321.

[20] Benito, M., Ortiz, I., Rodríguez, L., Muñoz, G. (2015). Ni–Co bimetallic catalyst for hydrogen production in sewage treatment plants: Biogas reforming and tars removal. *International Journal of Hydrogen Energy, 40*(42), pp. 14456 - 14468.

[21] Ramos, M. R. (2012). H_2 production with CO_2 capture by sorption enhanced chemical-looping reforming using NiO as oxygen carrier and CaO as CO_2 sorbent. *Fuel Processing Technology, 96*, pp. 27 - 36.

[22] Onwuemezie, L., Darabkhani, H. G., Ardekani, M. M. (2023). Hybrid solar-driven hydrogen generation by sorption enhanced–chemical looping and hydrocarbon reforming coupled with carbon capture and Rankine cycle. *International Journal of Hydrogen Energy, 48*(52), pp. 19936-19952.

[23] Su, B., Wang, Y., Xu, Z., Han, W., Jin, H., Wang, H. (2022). Novel ways for hydrogen production based on methane steam and dry reforming integrated with carbon capture. *Energy Conversion and Management, 270*, p. 116199.

[24] Onwuemezie, L., Darabkhani, H. G., Ardekani, M. M. (2023). Integrated solar-driven hydrogen generation by pyrolysis and electrolysis coupled with carbon capture and Rankine cycle. *Energy Conversion and Management, 277*, p. 116641.

[25] Rezaei, M., Mostafaeipour, A., Qolipour, M., Momeni, M. (2019). Energy supply for water electrolysis systems using wind and solar energy to produce hydrogen: a case study of Iran. *Frontiers in Energy, 13*, pp. 539 – 550.

[26] Nasser, M., Megahed, T. F., Ookawara, S., Hassan, H. (2022). A review of water electrolysis–based systems for hydrogen production using hybrid/solar/wind energy systems. *Environmental Science and Pollution Research, 29*, pp. 86994 – 87018.

[27] Karimi, R., Gheinani, T. T., Avargani, V. M. (2018). A detailed mathematical model for thermal performance analysis of a cylindrical cavity receiver in a solar parabolic dish collector system. *Renewable Energy, 125*, pp. 768 - 782.

[28] Azouzoute, A., Merrouni, A. A., Touili, S. (2020). Overview of the integration of CSP as an alternative energy source in the MENA region. *Energy Strategy Reviews, 29*, p. 100493.

[29] Kalogirou, S. A. (2014). *Solar Energy Engineering: Processes and Systems.* Academic Press.

[30] Sookramoon1, K., Bunyawanichakul1, P., Kongtragool, B. (2015). Experimental Study of a 2-stage Parabolic Dish-Stirling Engine in Thailand. *Walailak Journal, 13*(8), pp. 579 - 594.

[31] Uzair, M., Anderson, T., Nates, R. (2017). The impact of the parabolic dish concentrator on the wind induced heat loss from its receiver. *Solar Energy, 151*, pp. 95 - 101.

[32] Castellanos, L. S., Noguera, A. L., Caballero, G. E., Souza, A. L., Cobas, V. R., Lora, E. E., Venturini, O. J. (2019). Experimental analysis and numerical validation of the solar Dish/Stirling system connected to the electric grid. *Renewable Energy, 135*, pp. 259 - 265.

[33] Castellanos, L. S., Caballero, G. E., Cobas, V. R., Lora, E. E., Reyes, A. M. (2017). Mathematical modeling of the geometrical sizing and thermal performance of a Dish/Stirling system for power generation. *Renewable Energy, 107*, pp. 23 - 35.

[34] Holmes-Gentle, I., Tembhurne, S., Suter, C., Haussener, S. (2023). Kilowatt-scale solar hydrogen production system using a concentrated integrated photoelectrochemical device. *Nature Energy, 8*, pp. 586 – 596.

[35] Awan, A. B., Zubair, M., Praveen, R., Bhatti, A. R. (2019). Design and comparative analysis of photovoltaic and parabolic trough based CSP plants. *Solar Energy, 183*, pp. 551 - 565.

[36] Laha, P., Chakraborty, B. (2021). Low carbon electricity system for India in 2030 based on multi-objective multi-criteria assessment. *Renewable and Sustainable Energy Reviews, 135*, pp. 110356.

[37] Alderson, H., Cranston, G. R., Hammond, G. P. (2012). Carbon and environmental footprinting of low carbon UK electricity futures to 2050. *Energy, 48*(1), pp. 96 - 107.

[38] Deena, S. R., Vickram, A., Manikandan, S., Subbaiya, R., Karmegam, N., Ravindran, B., . . . Awasthi, M. K. (2022). Enhanced biogas production from food waste and activated sludge using advanced techniques – A review. *Bioresource Technology*, 355, p. 127234.

[39] Motte, J. C., Escudié, R., Bernet, N., Delgenes, J. P., Steyer, J. P., & Dumas, C. (2013). Dynamic effect of total solid content, low substrate/inoculum ratio and particle size on solid-state anaerobic digestion. *Bioresource Technology*, 144, pp. 141 – 148.

[40] Haider, A. R., Smith, J. (2018). *Process simulation and experimental investigation of biofuel production in a high rate anaerobic digestion process.* Doctoral Dissertations. 2664: https://scholarsmine.mst.edu/doctoral_dissertations/2664.

[41] Holtzapple, M. T., Wu, H., Weimer, P. J., Dalke, R., Granda, C. B., Mai, J., Urgun-Demirtas, M. (2022). Microbial communities for valorizing biomass using the carboxylate platform to produce volatile fatty acids: A review. *Bioresource Technology, 344*(Part B), p. 126253.

[42] Rosa, P. R., Santos, S. C., Sakamoto, I. K., Varesche, M. B., & Silva, E. L. (2014). Hydrogen production from cheese whey with ethanol-type fermentation: Effect of hydraulic retention time on the microbial community composition. *Bioresource Technology*, 161, pp. 10 – 19.

[43] Vu, H. P., Nguyen, L. N., Wang, Q., Ngo, H. H., Liu, Q., Zhang, X., Nghiem, L. D. (2022). Hydrogen sulphide management in anaerobic digestion: A critical review on input control, process regulation, and post-treatment. *Bioresource Technology, 346*, p. 126634.

[44] Hernández-Mendoza, C. E., Moreno-Andrade, I., & Buitrón, G. (2014). Comparison of hydrogen-producing bacterial communities adapted in continuous and discontinuous reactors. *International Journal of Hydrogen Energy*, 39(26), pp. 14234 – 14239.

[45] Preethi, Usman, T. M., Banu, J. R., Gunasekaran, M., & Kumar, G. (2019). Biohydrogen production from industrial wastewater: An overview. *Bioresource Technology Reports*, 7, p. 100287.

[46] Hajji, A., & Rhachi, M. (2022). The effect of thermochemical pretreatment on anaerobic digestion efficiency of municipal solid waste under mesophilic conditions. *Scientific African*, 16, p. e01198.

[47] Li, X.-H., Liang, D.-W., Bai, Y.-X., Fan, Y.-T., & Hou, H.-W. (2014). Enhanced H_2 production from corn stalk by integrating dark fermentation and single chamber microbial electrolysis cells with double anode arrangement. *International Journal of Hydrogen Energy*, 39(17), pp. 8977 – 8982.

[48] Lu, L., Ren, N., Xing, D., & Logan, B. E. (2009). Hydrogen production with effluent from an ethanol-H_2-coproducing fermentation reactor using a single-chamber microbial electrolysis cell. *Biosens Bioelectron*, 24(10), pp. 3055 – 3060.

[49] Kundu, A., Sahu, J. N., Redzwan, G., & Hashim, M. (2013). An overview of cathode material and catalysts suitable for generating hydrogen in microbial electrolysis cell. *International Journal of Hydrogen Energy*, 38(4), pp. 1745 – 1757.

[50] Kadier, A., Simayi, Y., Chandrasekhar, K., Ismail, M., & Kalil, M. S. (2015). Hydrogen gas production with an electroformed Ni mesh cathode catalysts in a single-chamber microbial electrolysis cell (MEC). *International Journal of Hydrogen Energy*, 40(41), pp. 14095 – 14103.

[51] Moore, T., Oyarzun, D. I., Li, W., Lin, T. Y., Goldman, M., Wong, A. A., . . . Hahn, C. (2023). Electrolyzer energy dominates separation costs in state-of-the-art CO_2 electrolyzers: Implications for single-pass CO_2 utilization. *Joule*, 7(4), pp. 782 – 796.

[52] Cleiren, E., Heijkers, S., Ramakers, M., & Bogaerts, A. (2017). Dry Reforming of Methane in a Gliding Arc Plasmatron: Towards a Better Understanding of the Plasma Chemistry. *Chemistry-Sustainability-Energy-Materials*, 10(20), pp. 4025 – 4036.

[53] Guo, X. M., Trably, E., Latrille, E., Carrère, H., Steyer, J. P. (2010). Hydrogen production from agricultural waste by dark fermentation: A review. *International Journal of Hydrogen Energy*, *35*(19), pp. 10660 - 10673.

[54] Wang, N., Chui, C., Zhang, S., Liu, Q., Li, B., Shi, J., & Liu, L. (2022). Hydrogen Production by the Thermophilic Dry Anaerobic Co-Fermentation of Food Waste Utilizing Garden Waste or Kitchen Waste as Co-Substrate. *Sustainability*, 14(12), p. 7367.

[55] Subramani, J., Nagarajan, P., Subramaniyan, C., & Anbuselvan, N. (2021). Performance studies on solar parabolic dish collector using conical cavity receiver for community heating applications. Materialtoday: *Proceedings*, 45(1), pp. 1862 – 1866.

[56] Ozgener, O. (2006). A small wind turbine system (SWTS) application and its performance analysis. *Energy Conversion and Management*, 47(11 - 12), pp. 1326 – 1337.

[57] Maghami, M. R., Hizam, H., Gomes, C., Radzi, M. A., Rezadad, M. I., & Hajighorbani, S. (2016). Power loss due to soiling on solar panel: A review. *Renewable and Sustainable Energy Reviews*, 59, pp. 1307 – 1316.

[58] Calbry-Muzyka, A., Madi, H., Rüsch-Pfund, F., Gandiglio, M., & Biollaz, S. (2022). Biogas composition from agricultural sources and organic fraction of municipal solid waste. *Renewable Energy*, 181, pp. 1000 – 1007.

[59] Onwuemezie, L., Darabkhani, H. G., & Montazeri-Gh, M. (2024). Pathways for low carbon hydrogen production from integrated hydrocarbon reforming and water electrolysis for oil and gas exporting countries. *Sustainable Energy Technologies and Assessments*, 61, p. 103598.

[60] Argyris, P. A., Wong, J., Wright, A., Pereira, L. M., & Spallina, V. (2023). Reducing the cost of low-carbon hydrogen production via emerging chemical looping process. *Energy Conversion and Management*, 277, p. 116581.

[61] Jia, J., Seitz, L. C., Benck, J. D., Huo, Y., Chen, Y., Ng, J. W., . . . Jaramillo, T. F. (2016). Solar water splitting by photovoltaic-electrolysis with a solar-to-hydrogen efficiency over 30%. *Nature Communications*, p. 13237.

[62] Jia, Y. H., Ryu, J. H., Kim, C. H., Lee, W. K., Tran, T. V., Lee, H. L., . . . Ahn, D. H. (2012). Enhancing hydrogen production efficiency in microbial electrolysis cell with membrane electrode assembly cathode. *Journal of Industrial and Engineering Chemistry*, 18(2), pp. 715 – 719.

[63] Lee, D. H. (2021). Biohydrogen yield efficiency and the benefits of dark, photo and dark-photo fermentative production technology in circular Asian economies. *International Journal of Hydrogen Energy*, 46(27), pp. 13908 – 13922.

[64] Kang, D., Saha, S., Kurade, M. B., Basak, B., Ha, G.-S., Jeon, B.-H., . . . Kim, J. R. (2021). Dual-stage pulse-feed operation enhanced methanation of lipidic waste during co-digestion using acclimatized consortia. *Renewable and Sustainable Energy Reviews*, 145, p. 111096.

[65] Liu, C., Wang, W., Anwar, N., Ma, Z., Liu, G., & Zhang, R. (2017). Effect of Organic Loading Rate on Anaerobic Digestion of Food Waste under Mesophilic and Thermophilic Conditions. *Energy Fuels*, 31, pp. 2976 – 2984.

[66] Shehzad, A., Bashir, M. J., & Sethupathi, S. (2016). System analysis for synthesis gas (syngas) production in Pakistan from municipal solid waste gasification using a circulating fluidized bed gasifier. *Renewable and Sustainable Energy Reviews*, 60, pp. 1302 – 1311.

[67] Yazdanifard, F., Ebrahimnia-Bajestan, E., & Ameri, M. (2016). Investigating the performance of a water-based photovoltaic/thermal (PV/T) collector in laminar and turbulent flow regime. *Renewable Energy*, 99, pp. 295 – 306.

[68] Ji, J., Zhang, J., Yang, L., He, Y., Zhang, R., Liu, G., & Chen, C. (2017). Impact of co-pretreatment of calcium hydroxide and steam explosion on anaerobic digestion efficiency with corn stover. *Environmental Technology*, 38(12), pp. 1465 – 1473.

[69] Ma, S., Wang, H., Li, L., Gu, X., & Zhu, W. (2021). Enhanced biomethane production from corn straw by a novel anaerobic digestion strategy with mechanochemical pretreatment. *Renewable and Sustainable Energy Reviews*, 146, p. 111099.

[70] Aiken, D. C., Curtis, T. P., & Heidrich, E. S. (2019). Avenues to the financial viability of microbial electrolysis cells [MEC] for domestic wastewater treatment and hydrogen production. *International Journal of Hydrogen Energy*, 44(1), pp. 2426 – 2434.

[71] Pant, D., Bogaert, G. V., Smet, M. D., Diels, L., & Vanbroekhoven, K. (2012). Use of novel permeable membrane and air cathodes in acetate microbial fuel cells. *Electrochimica Acta*, 55(6), pp. 7710 – 7716.

[72] Zhang, Y., Matthew, Merrill, M. D., & Logan, B. E. (2010). The use and optimization of stainless steel mesh cathodes in microbial electrolysis cells. *International Journal of Hydrogen Energy*, 35(21), pp. 12020 – 12028.

[73] Ghasemi, M., Shahgaldi, S., Ismail, M., Yaakob, Z., & Daud, W. R. (2012). New generation of carbon nanocomposite proton exchange membranes in microbial fuel cell systems. *Chemical Engineering Journal*, pp. 184, 82 – 89.

[74] Aiken, D. C., Curtis, T. P., & Heidrich, E. S. (2022). The Rational Design of a Financially Viable Microbial Electrolysis Cell for Domestic Wastewater Treatment. *Frontiers in Chemical Engineering*, 3.

[75] Krishnan, S., Koning, V., Groot, M. T., Groot, A. d., Mendoza, P. G., Junginger, M., & Kramer, G. J. (2021). Present and future cost of alkaline and PEM electrolyser stacks. *International Journal of Hydrogen Energy*, 48(83), pp. 32313 – 32330.

[76] Oreggioni, G. D., Gowreesunker, B. L., Tassou, S. A., Bianchi, G., Reilly, M., Kirby, M. E., . . . Theodorou, M. K. (2017). Potential for Energy Production from Farm Wastes Using Anaerobic Digestion in the UK: An Economic Comparison of Different Size Plants. *Energies*, 10(9), p.1396.

[77] Carlini, M., Mosconi, E. M., Castellucci, S., Villarini, M., & Colantoni, A. (2017). An Economical Evaluation of Anaerobic Digestion Plants Fed with Organic Agro-Industrial Waste. *Energies*, 10(8), p. 1165.

[78] Ibarra-Esparza, F. E., González-López, M. E., Ibarra-Esparza, J., Lara-Topete, G. O., Senés-Guerrero, C., Cansdale, A., . . . Gradilla-Hernández, M. S. (2023). Implementation of anaerobic digestion for valorizing the organic fraction of municipal solid waste in developing countries: Technical insights from a systematic review. *Journal of Environmental Management*, 347, p. 118993.

[79] Thi, N. B., Lin, C. Y., & Kumar, G. (2016). Electricity generation comparison of food waste-based bioenergy with wind and solar powers: A mini review. *Sustainable Environment Research*, 26(5), pp. 197 – 202.

[80] Steinberg, M., & Cheng, H. C. (1989). Modern and prospective technologies for hydrogen production from fossil fuels. *International Journal of Hydrogen Energy*, 14(11), pp. 797 – 820.

[81] Parkinson, B., Matthews, J. W., McConnaughy, T. B., Upham, D. C., & McFarland, E. W. (2017). Techno-Economic Analysis of Methane Pyrolysis in Molten Metals: Decarbonizing Natural Gas. *Chemical Engineering & Technology*, 40(6), pp. 1022 – 1030.

[82] Silva, H. N., Prata, D. M., Lima, G. B., Zotes, L. P., & Mattos, L. V. (2018). A techno-economic evaluation of the energy generation by proton exchange membrane fuel cell using biogas reforming. *Journal of Cleaner Production*, 200, pp. 598 – 608.

[83] Lilliestam, J., & Pitz-Paal, R. (2018). Concentrating solar power for less than USD 0.07 per kWh: finally the breakthrough. *Renewable Energy Focus*, 26, pp. 17 – 21.

[84] Xu, Y., Pei, J., Yuan, J., & Zhao, G. (2021). Concentrated solar power: technology, economy analysis, and policy implications in China. *Environmental Science and Pollution Research*, 29, pp. 1324 – 1337.

[85] Singh, V. P., Vijay, V., H.a, G. S., Chaturvedi, D. K., & Rajkumar, N. (2013). Analysis of solar power variability due to seasonal variation and its forecasting for Jodhpur region using Artificial Neural Network. *CPRI*, 9(3), pp. 140 – 148.

[86] Tiwary, A., Williams, I., Pant, D., Kishore, V. (2015). Emerging perspectives on environmental burden minimisation initiatives from anaerobic digestion technologies for community scale biomass valorisation. *Renewable and Sustainable Energy Reviews*, *42*, pp. 883 - 901.